JEM

Article

Continuous activity of Foxo1 is required to prevent anergy and maintain the memory state of CD8$^+$ T cells

Arnaud Delpoux,[1,2] Rodrigo Hess Michelini,[1,2] Shilpi Verma,[3] Chen-Yen Lai,[1,2] Kyla D. Omilusik,[1] Daniel T. Utzschneider,[1,2] Alec J. Redwood,[4] Ananda W. Goldrath,[1] Chris A. Benedict,[3] and Stephen M. Hedrick[1,2]

[1]Molecular Biology Section, Division of Biological Sciences, University of California, San Diego, La Jolla CA
[2]Cellular and Molecular Medicine, University of California, San Diego, La Jolla, CA
[3]Division of Immune Regulation, La Jolla Institute for Allergy and Immunology, La Jolla, CA
[4]Institute for Immunology and Infectious Diseases, Murdoch University, Murdoch, Western Australia, Australia

Upon infection with an intracellular pathogen, cytotoxic CD8$^+$ T cells develop diverse differentiation states characterized by function, localization, longevity, and the capacity for self-renewal. The program of differentiation is determined, in part, by FOXO1, a transcription factor known to integrate extrinsic input in order to specify survival, DNA repair, self-renewal, and proliferation. At issue is whether the state of T cell differentiation is specified by initial conditions of activation or is actively maintained. To study the spectrum of T cell differentiation, we have analyzed an infection with mouse cytomegalovirus, a persistent-latent virus that elicits different cytotoxic T cell responses characterized as acute resolving or inflationary. Our results show that FOXO1 is continuously required for all the phenotypic characteristics of memory-effector T cells such that with acute inactivation of the gene encoding FOXO1, T cells revert to a short-lived effector phenotype, exhibit reduced viability, and manifest characteristics of anergy.

Journal of Experimental Medicine

INTRODUCTION

Immune memory is usually studied in the context of reinfection after clearance of an acutely infectious agent. At some point after the primary infection, the immune system returns to relative quiescence, but upon reinfection, there occurs a secondary or anamnestic response that is faster and more robust. This immunity arises as a result of increased precursor frequencies and functional changes in antigen-specific T and B cells and the presence of preformed specific antibodies. The long-lived antigen-specific T cells are retained in secondary lymphoid organs, in vascular circulation, and embedded in various organs as tissue-resident memory T cells (Masopust et al., 2001; Sallusto et al., 2004; Obar and Lefrançois, 2010; Steinert et al., 2015).

Many infectious agents have "adopted" persistence as a strategy to remain endemic within a host population. Such microbes and viruses are never completely cleared from the body, and thus, the immune system is indefinitely exposed to antigenic stimulation. As such, the notion of primary and secondary responses does not apply. Some examples of viral persistence are met with diminished T cell reactivity characterized as exhaustion (Zajac et al., 1998; Day et al., 2006; Urbani et al., 2006; Wherry et al., 2007; Gigley et al., 2012; Barathan et al., 2015). Nonetheless, in all instances where this has been examined, such T cell populations play a continuing role in controlling the infectious agent (Zehn et al., 2016). In other examples, such as the latency of α-, β-, or γ-herpesviruses, persistence is not associated with the typical characteristics of exhausted T cells, even though evidence shows that there is continuous antigenic stimulation (Klenerman and Hill, 2005; Seckert et al., 2012).

The initial bias to form short-lived effector T cells versus long-lived memory T cells may occur as early as the first division of naive CD8$^+$ T cells after antigen presentation (Chang et al., 2007). The daughter cell proximal to the antigen-presenting cell expresses MYC, preferentially activates the mTOR pathway, and its progeny exhibit metabolic and functional characteristics of effector cells. The distal daughter cell is more likely to exhibit characteristics of memory T cells (Pollizzi et al., 2016; Verbist et al., 2016). Another arc of investigation has shown a role for FOXO1 in CD8$^+$ T cell memory, where inactivation of the *Foxo1* gene almost entirely prevented a secondary memory response (Rao et al., 2012; Hess Michelini et al., 2013; Kim et al., 2013). Because MYC can be antagonized by the transcription factor FOXO1 or FOXO3 (Peck et al., 2013; Tan et al., 2015; Wilhelm et al., 2016), a proposal is that differential activity of FOXO1 determines, in part, the initial outcome of effector versus memory specification (Verbist et al., 2016). Consistent with this notion, an analysis of T cells early in an infection showed

Correspondence to Stephen M. Hedrick: shedrick@ucsd.edu

R. Hess Michelini's present address is Genomics Institute of the Novartis Research Foundation, San Diego, CA.

S. Verma's present address is BD Biosciences, La Jolla, CA.

The Rockefeller University Press
J. Exp. Med. 2018 Vol. 215 No. 2 575–594
https://doi.org/10.1084/jem.20170697

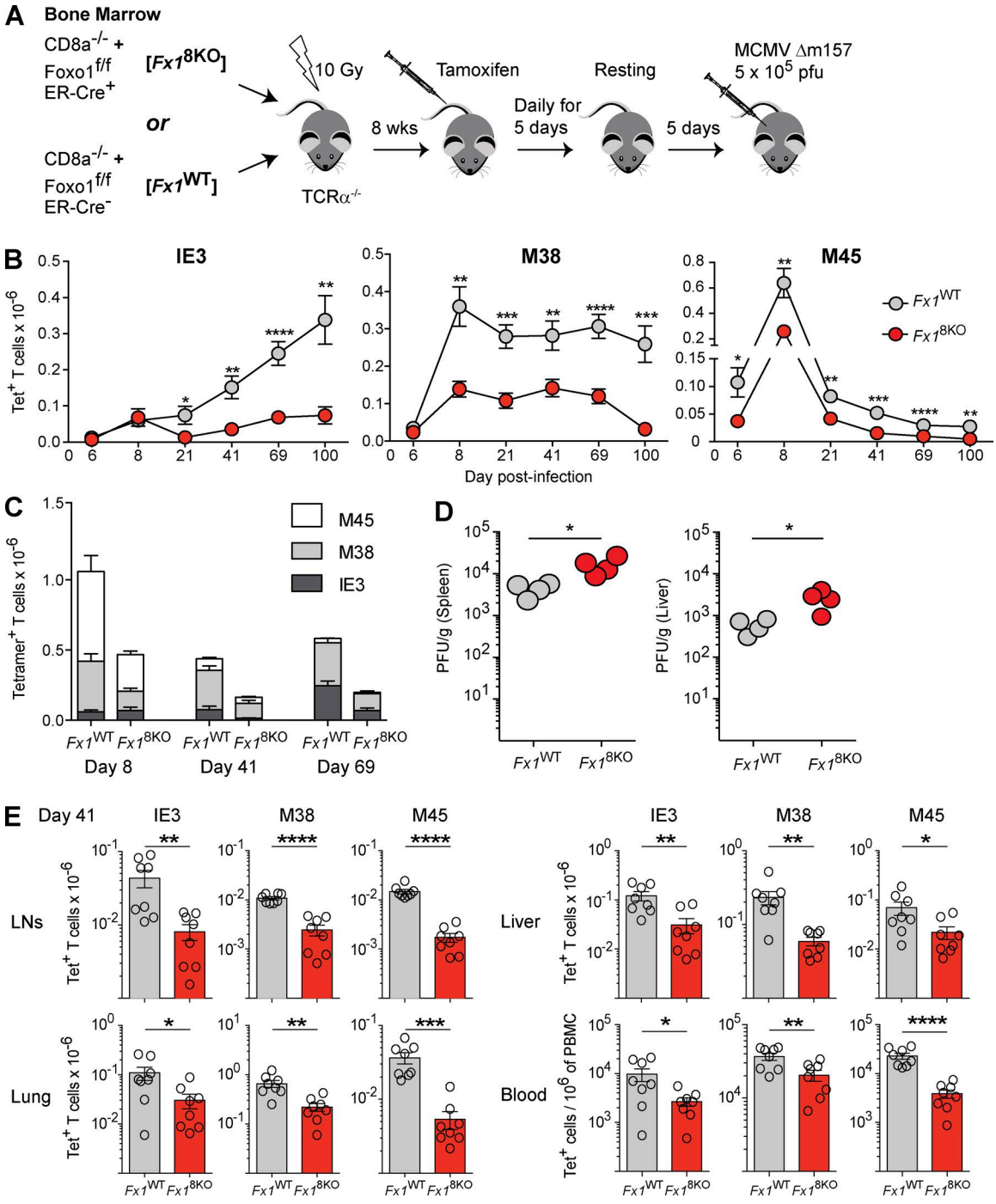

Figure 1. **MCMV-specific CD8⁺ T cell responses are compromised in *Fx1*^{8KO} mice. (A)** Model of bone marrow chimeras, tamoxifen treatment, and infection with MCMV-Δm157. **(B)** Accumulated data showing the course of T cell expansion and contraction over the course of infection. **(C)** Histograms represent the proportion in number of CD8⁺ T cells (IE3, M38, and M45) at 8, 41, and 69 dpi in the spleen. Data in B and C are cumulative from two experiments for days 6 and 100, three experiments for days 8 and 21, and five experiments for day 41 and 69 with three to five mice per group and per time point for each experiment. **(D)** Viral titers were determined by plaque assay in the spleen and the liver at day 6 after infection. Data represent one experiment with four mice per group. **(E)** Histograms represent the number of tetramer⁺ T cells for each epitope in LNs, lungs, liver, and blood at day 41 after infection. Data are cumulative from two experiment with $n = 4$ mice per group and per experiment. *, $P < 0.05$; **, $P < 0.01$; ***, $P < 0.001$; ****, $P < 0.0001$ (unpaired Student's *t* test); error bars represent mean ± SEM.

that almost 90% of the gene expression specific to memory precursor cells was diminished in the absence of FOXO1 (Hess Michelini et al., 2013). The importance of this finding is that FOXO transcription factors are dynamically regulated by many posttranslational modifications signaled by extrinsic input to the cell: the availability of growth factors and nutrients or the presence of inflammation or oxidative stress (Calnan and Brunet, 2008). Thus, a possibility is that the state of T cell differentiation itself is plastic and actively determined by the changing environment of a responding T cell.

In this study, we have investigated two issues related to T cell memory differentiation. First, within the diversity of long-lived T cells that arise as a result of a β-herpesvirus infection, are there differential requirements for FOXO1 depending on the kinetics and phenotypic characteristics of the responding T cells? Second, is the state of effector versus memory T cells permanently determined early in an infection, or must it be continuously maintained? Our studies reveal that T cell responses, defined by epitope recognition, were uniformly sensitive to the loss of FOXO1. With a loss of *Foxo1*, T cells expanded at a reduced rate, were deficient for effector cytokines, and exhibited characteristics of anergy. In addition, the results show that a memory phenotype must be actively maintained by the presence of FOXO1; upon inactivation of *Foxo1*, memory T cells reverted to a state reminiscent of terminally differentiated effector T cells. The analysis provides a unique window into T cell differentiation and the complex interplay between short-lived effector T cells and long-term memory that develops in the presence of sustained antigens.

RESULTS

Foxo1 is required for antigen-specific T cell expansion in response to MCMV

To study the role of FOXO1 in the response to murine cytomegalovirus (MCMV), we produced radiation chimeric mice that provided a means of acutely deleting *Foxo1* in $CD8^+$ T cells. Bone marrow from either $Foxo1^{f/f}$ ER-Cre^+ ($Fx1^{8KO}$ chimera) or $Foxo1^{f/f}$ ER-Cre^- ($Fx1^{WT}$ chimera) mice was mixed with bone marrow from $Cd8a^{-/-}$ mice and used to repopulate $Tcra^{-/-}$ mice ablated by lethal irradiation. After treatment with tamoxifen, only the $Foxo1^{-/-}$ $CD8^+$ ($Fx1^{8KO}$) T cells are not complemented by WT bone marrow cells (Fig. 1 A). We note that this differs from our previous experimental model in which *Foxo1* was not deleted until after the T cells became activated (Hess Michelini et al., 2013). Chimeras were inoculated with MCMV Δm157 that lacks the ligand recognized by $Ly49H^+$ NK cells because we wanted to focus on the cytotoxic T cell response, and most inbred and outbred mouse strains lack Ly49H (Brown et al., 2001; Arase et al., 2002; Smith et al., 2002; Scalzo et al., 2005).

Using antigen-specific tetramer staining, we analyzed T cell populations that recognize three immunodominant MCMV epitopes displaying distinct expansion and contraction kinetics (Fig. S1 A; Munks et al., 2006). As previously described, T cells that recognized the IE3 epitope, termed inflationary, showed very modest initial expansion but accumulated steadily over the course of 100 d. T cells that recognized M38 rapidly expanded over the first week but did not contract until more than 69 d after infection. In contrast, T cells that recognized the M45 epitope displayed kinetics typical of an acute viral infection: rapid expansion over the first week followed by equally rapid contraction (Fig. 1 B).

Within the population of $Fx1^{8KO}$ T cells, there was a three- to fourfold reduction in the number of accumulated T cells throughout the course of the experiment, and yet the unique kinetic profile for each of these responses was retained. FOXO1 was necessary for both the initial acute expansion exemplified by M45-specific T cells and the slow inflation exemplified by IE3-specific T cells with no effect on the profile of contraction (Fig. 1 B). This is also depicted by the changing contribution of epitope-specific T cells over the course of the response (Fig. 1 C), and similar kinetics were found for T cells in the liver (Fig. S1 B). In addition, we found no differences in the numbers of dendritic cells (DCs), total $CD4^+$ T cells or regulatory T cells (T reg cells; Fig. S1 C), and remarkably, virtually all of these cells were $FOXO1^+$ (not depicted). This indicates that WT DCs, B cells, and $CD4^+$ T cells outcompeted the equivalent $Foxo1^{-/-}$ cells. In addition, this inactivation of *Foxo1* in $CD8^+$ T cells had a modest but significant effect on the initial viral load in both the spleen and liver at 6 d after infection (Fig. 1 D). The efficiency of *Foxo1* inactivation was verified in all $tetramer^+$ cells at day 8 after infection and through the end of the experiments (day 69 after infection; Fig. S1 D and not depicted). We further determined whether the loss FOXO1 affected the MCMV-specific $CD8^+$ T cell response in other organs. At day 41 after infection, the numbers of $Fx1^{8KO}$ T cells were reduced in lung, liver, and blood as well as lymph nodes (Fig. 1 E). Altogether, these data show an important role of FOXO1 for the maximal expansion of MCMV-specific $CD8^+$ T cells specific for different viral epitopes.

Foxo1 is required for ongoing $CD8^+$ T cell survival

To examine the origin of the diminished populations of T cells, the proportion of cells in cell cycle was determined by the expression of Ki67, a nucleolar protein not expressed in G_o quiescent cells (Gerdes et al., 1984; Kill, 1996). There was no difference in the proportion of $Fx1^{8KO}$ versus $Fx1^{WT}$ T cells in cycle at early or late time points (Fig. 2 A), and this suggested that the deficiency in T cell accumulation may be caused by a loss of viability. Consistent with BCL2 as an important survival factor that is induced in memory T cells (Wojciechowski et al., 2007; Kurtulus et al., 2011), we found that *Foxo1*-null T cells specific for all three epitopes expressed substantially lower amounts of BCL2 compared with $Fx1^{WT}$ T cells in the spleen and liver (Fig. 2 B and Fig. S2, A and B).

To enumerate apoptotic T cells, $tetramer^+$ cells were analyzed for cell-surface Annexin V binding (Fig. 2 C) and intracellular cleaved caspase-3 (Fig. 2 D). Both measures revealed a large increase in apoptotic or potentially apoptotic

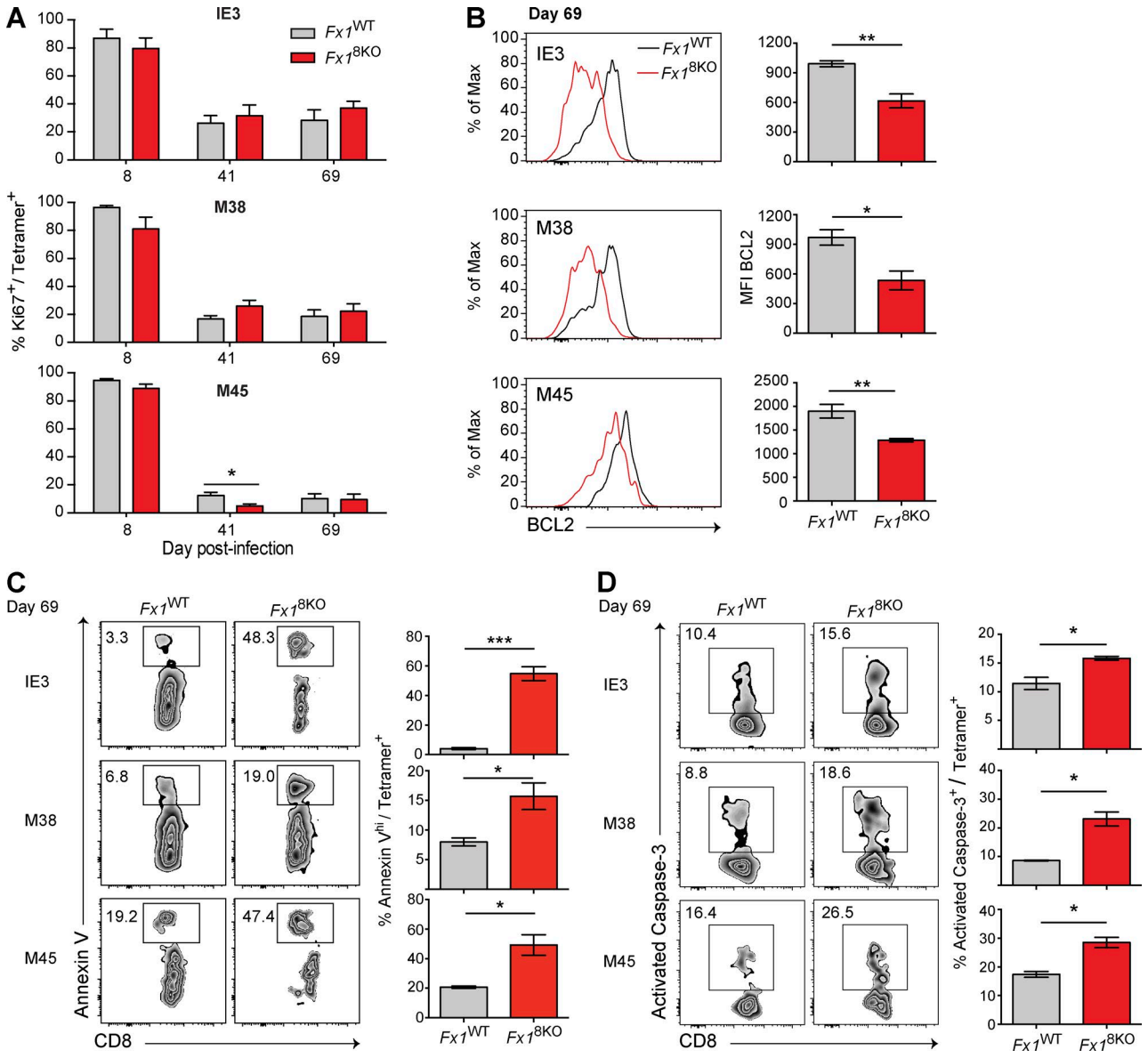

Figure 2. **MCMV-specific *Fx1*^{8KO} CD8$^+$ T cells are more prone to apoptosis. (A–D)** *Fx1*^{WT} and *Fx1*^{8KO} splenocytes specific for each of the three tetramers were recovered at various times and analyzed for the expression of cell-surface or intracellular molecules as indicated. (A) Histograms bar represent the percentage of Ki67+ per tetramer at different time point. (B) FACS histograms represent the expression of BCL2 at day 69 after infection. Quantifications of BCL2 MFI were plotted for each tetramer. (C and D) FACS dot plot represent the expression of Annexin V (C) and activated caspase-3 (D). Numbers represent the percentage of Annexin V$^+$ and activated caspase-3$^+$ T cells, respectively. Data are cumulative from two experiments for (A, B, and D) with $n = 3$ or 4 mice per group and one experiment for (C) with $n = 3$ or 4 mice per group. *, $P < 0.05$; **, $P < 0.01$; ***, $P < 0.001$ (unpaired Student's *t* test); error bars represent mean ± SEM.

cells found in *Fx1*^{8KO} versus *Fx1*^{WT} T cells starting at day 8 and all time points hence (Fig. S2 C). Moreover, an increase of apoptotic cells in *Fx1*^{8KO} was also observed in the LNs and lung (Fig. S2, D and E). Even during the contraction phase of M45-specific T cells, FOXO1 was required for T cell viability. Although in some contexts it can cause apoptosis (Brunet et al., 1999), these data suggest that FOXO1 is required to sustain the viability of Ag-specific CD8$^+$ T cells at all phases of the response. Simplistically, an increased rate of death would be expected to cause a progressive decrease in the relative number of Fx1 cells; however, the ratio of WT:KO T cells remains constant, and thus there may be other homeostatic effects on the total number of T cells.

Foxo1-null T cells exhibit anergy, but not checkpoint-specific exhaustion

The functional capability of T cells strongly correlates with their ability to produce multiple cytokines, especially the ef-

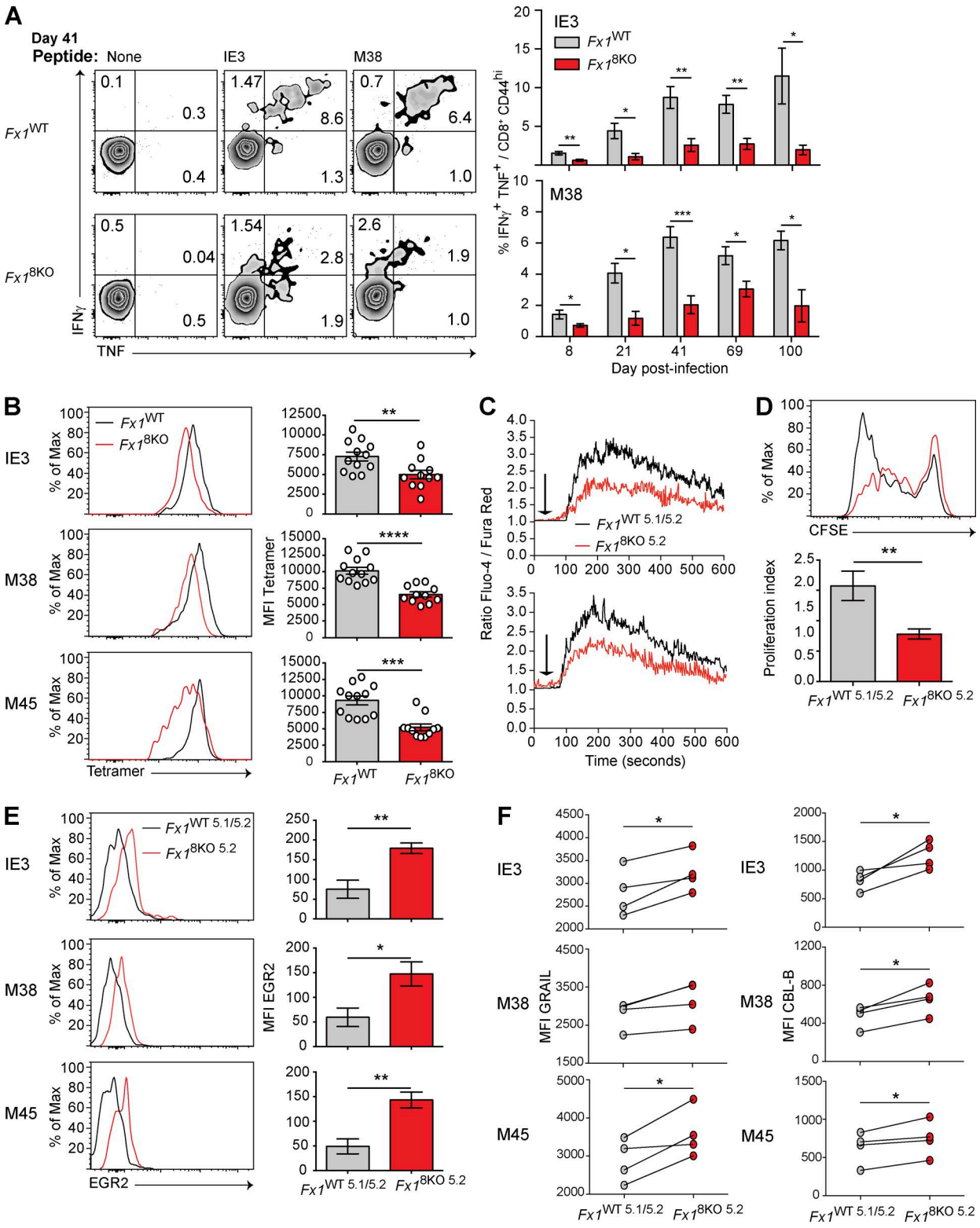

Figure 3. **Inflationary *Fx1*^{8KO} CD8$^+$ T cells are deficient for effector cytokines and display an anergic state. (A)** Splenocytes from *Fx1*^{WT} and *Fx1*^{8KO} chimeras were harvested at different time points after infection, and total splenocytes were stimulated for 5 h with or without specific peptide. Bivariant analysis of IFNγ and TNF at 41 dpi gated on CD8$^+$ CD44^{hi} cells (left) and graphed for each time point (right). Numbers represent the percentage of IFNγ$^+$ TNF$^-$, IFNγ$^+$ TNF$^+$ or IFNγ$^-$ TNF$^+$. **(B)** Histogram of tetramer expression and the MFI plotted for T cells specific for each epitope. Data in A and B are cumulative from 3 experiments with $n = 4$ mice for each group per experiment and per time point. **(C)** Curves show ratio of Fluo-4 MFI and FuraRed MFI over time. At 30 s,

fector cytokines IFNγ and TNF (Wherry et al., 2003; Betts et al., 2006). *Fx1*^{WT} or *Fx1*^{8KO} T cells from MCMV-infected chimeras were stimulated with either IE3 or M38 peptide, and examined for the coexpression of IFNγ and TNF. Whereas most of the cytokine-producing WT T cells produced both IFNγ and TNF, the total percentage of cytokine-producing *Fx1*^{8KO} T cells was diminished, and these cells were equally distributed between single and double cytokine production (Fig. 3 A, left). This diminution of double cytokine producing T cells was characteristic of T cells throughout the course of the response (Fig. 3 A, right; and Fig. S3 A), and it was also reflected in the intensity of IFNγ expression per cell (Fig. S3 B).

Unlike the response to chronic LCMV infection, infection with MCMV or other herpesviruses does not appear to cause the responding T cell populations to induce cell-surface molecules characteristic of negative feedback regulation often referred to as "exhaustion" (Day et al., 2006; Urbani et al., 2006). How these persistent and latent virus infections fundamentally differ is unclear, but we sought to determine whether the lack of FOXO1 would alter this phenotype. As depicted in Fig. S3 C, there was no indication that any of the receptors typical of exhaustion were expressed on T cells from either genotype. This included PD-1, LAG-3, TIM-3, and CTLA-4. However, we noticed that there was a consistent decrease in tetramer binding in *Fx1*^{8KO} T cells (Fig. 3 B) without a concomitant decrease in CD3ε (not depicted). This lower receptor avidity for antigen-MHC binding has been found in anergic CD4$^+$ T cells (Mallone et al., 2005; Maeda et al., 2014) and CD8$^+$ T cells recently activated with antigen (Drake et al., 2005). The diminished tetramer binding was caused by TCR redistribution, but not changes in receptor affinity. Similarly, we find that the reduced tetramer binding does not reflect a difference in TCR affinity as measured by a M38 tetramer decay assay (Fig. S3 G).

To study the role of FOXO1 in the anergy induction, we produced mixed chimeric mice in which bone marrow cells from *Foxo1*$^{f/f}$ ER-Cre$^+$ CD45.2 (*Fx1*$^{8KO\ 5.2}$ chimera) and C57BL/6 CD45.1/CD45.2 (*Fx1*$^{WT\ 5.1/5.2}$ chimera) mice were used to repopulate C57BL/6 CD45.1 mice ablated by lethal irradiation. This model allowed us to study the behavior of the *Foxo1*-null CD8$^+$ T cells in a competition with the WT CD8$^+$ T cells (Fig. S3 D). We note, in this competitive model, the number of *Fx1*$^{8KO\ 5.2}$ MCMV-specific CD8$^+$ T cells was again reduced over the time of infection for all three epitopes (not depicted).

A hallmark of T cell anergy is a loss of sensitivity to stimulation through the T cell antigen receptor complex as measured by proximal signaling (Dubois et al., 1998). The total antigen-reactive T cell populations from the spleen of chimeras with both *Fx1*$^{WT\ 5.1/5.2}$ and *Fx1*$^{8KO\ 5.2}$ T cells were stimulated by cross-linking CD3ε and the release of free calcium was measured over time. As shown, the calcium release was attenuated in *Fx1*$^{8KO\ 5.2}$ T cells compared with *Fx1*$^{WT\ 5.1/5.2}$ T cells (Fig. 3 C) in the same culture, and this attenuated signaling manifested in reduced proliferation (Fig. 3 D).

This signaling defect also correlated with a reduced activation of NFAT1,2 (Fig. S3 E). In addition, the transcription factor EGR2 and three E3 ligases, GRAIL, CBL-B, and ITCH, have been associated with anergy, and all four were increased in *Fx1*$^{8KO\ 5.2}$ T cells (Fig. 3, E and F; and Fig. S3 F; Jeon et al., 2004; Safford et al., 2005; Whiting et al., 2011; Oh et al., 2015). Collectively, these data demonstrate that FOXO1 expression is required to prevent the induction of anergy in Ag-specific CD8$^+$ T cells that arise in response to MCMV infection.

Transcriptional control is dysregulated in the absence of Foxo1

CD27 is a TNF-family receptor member that serves as a coreceptor for T cell activation, marks memory precursors, and specifically promotes the inflationary T cell expansion in response to MCMV infection (Borst et al., 2005; Welten et al., 2015). Analysis of *Fx1*^{WT} T cells showed that bivariant plots of KLRG1 versus CD27 reveals that these two cell surface molecules are largely expressed on distinct subsets after infection. The inflationary T cells specific for IE3 or M38 predominantly show characteristics of effector T cells, whereas the acutely reactive M45-specific T cells are more evenly divided between putative effector and memory-effector T cells. However, a loss of FOXO1 affects acute and inflationary T cells similarly at late time points, in each case exaggerating effector characteristics (Fig. 4, A and B). The use of CD27 to delineate a memory cell phenotype was further indicated by an analysis of ID3 expression, a characteristic of memory T cells (Yang et al., 2011; Fig. 4 C).

As a counterpart to ID3 in memory T cells, TBET (TBX21) is a key transcription factor in the induction of effector T cells (Rutishauser and Kaech, 2010), and previous work has shown that its down-regulation depends on the expression of FOXO1 (Kerdiles et al., 2010; Rao et al., 2012).

anti–hamster antibody was added (arrow). The curves represent the CD8$^+$ CD44^{hi} CD11a^{hi} T cells for *Fx1*$^{WT\ 5.1/5.2}$ and *Fx1*$^{8KO\ 5.2}$ cells. Data are representative of two experiments with three mice each (n = 6; two mice shown). **(D)** Total CD8$^+$ T cells from *Fx1*$^{WT\ 5.1/5.2}$ chimeras and *Fx1*$^{8KO\ 5.2}$ chimeras were isolated from the spleen and activated for 3 d with plate-bound CD3- and CD28-specific antibodies. CFSE profiles are shown for CD8$^+$ T cells gated on CD45.1$^+$ CD45.2$^+$ and CD45.2$^+$ CD45.1$^-$ for *Fx1*$^{WT\ 5.1/5.2}$ (black) and *Fx1*$^{8KO\ 5.2}$ (red), respectively. Data are representative of three independent experiments. Proliferation index was calculated from three independent experiments with three mice per experiment. **(E and F)** Egr2 (E) and Grail and Cbl-b (F) intracellular expression was determined and the MFI plotted for T cells specific for each epitope. Data in E are cumulative from two experiments with n = 3 or 4 mice per group. In F, one representative experiment is shown from two experiments with four mice. *, P < 0.05; **, P < 0.01; ***, P < 0.001; ****, P < 0.0001 (unpaired [A and B] or paired [D–F] Student's t test); error bars represent mean ± SEM.

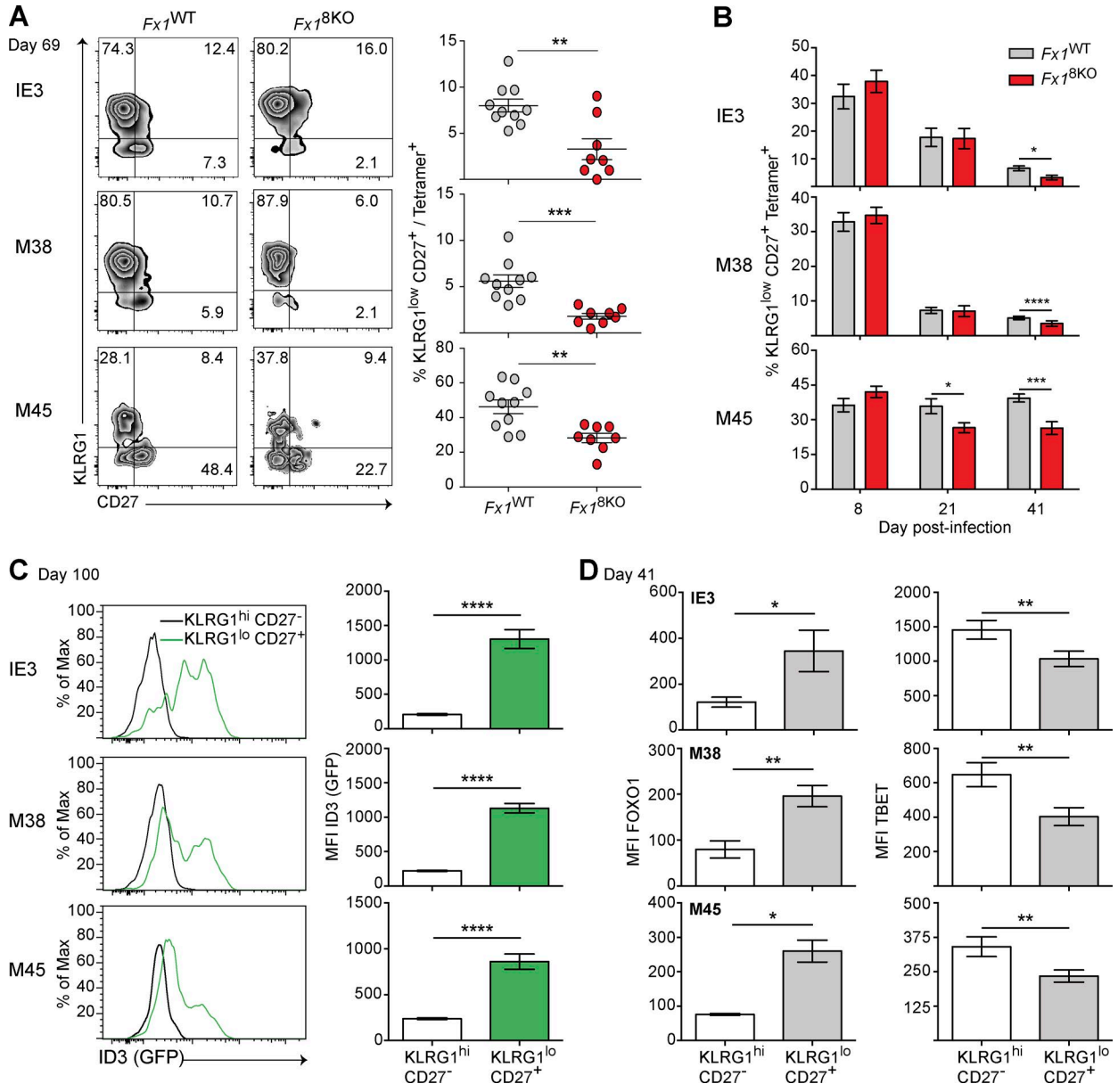

Figure 4. **Ag-specific *Fx1*^{8KO} CD8$^+$ T cells produce fewer memory precursors. (A)** Spleen from *Fx1*^{WT} and *Fx1*^{8KO} chimeras were harvested at 69 dpi, and tetramer$^+$ cells were examined for the expression of KLRG1 and CD27. Graphs represent the quantification of the percentage of KLRG1^{low} CD27$^+$. Data are cumulative from three independent experiments with $n = 2$ to 4 mice per experiment and per group. **(B)** Histograms represent the percentage of KLRG1^{low} CD27$^+$ for each tetramer at day 8, 21, and 41 after infection. Data are cumulative from two to four experiments with minimum $n = 3$ mice per group and per time point. **(C)** Spleens from ID3-GFP reporter mice were harvested at day 100 after infection and the expression of ID3 was examined on KLRG1^{low} CD27$^+$ and KLRG1^{hi} CD27$^-$ for each tetramer. Data are from one experiment with four mice. **(D)** Spleens from *Fx1*^{WT} chimeras were harvested at 41 after infection and the expression of FOXO1 and TBET was examined on KLRG1^{low} CD27$^+$ and KLRG1^{hi} CD27$^-$ cells for each tetramer. Data are from one experiment with five mice. *, $P < 0.05$; **, $P < 0.01$; ***, $P < 0.001$; ****, $P < 0.0001$ (unpaired [A and B] or paired [C and D] Student's t test); error bars represent mean ± SEM.

Indeed, whereas FOXO1 is relatively high in memory precursor cells (KLRG1^{lo}CD27^{hi}), TBET is relatively low (Fig. 4 D).

Loss of *Foxo1* prevents expression of the HMG-box transcription factor TCF7 (alias TCF-1; Hess Michelini et al., 2013; Kim et al., 2013), a part of the canonical Wingless/Integration 1 (Wnt) signaling pathway (Clevers, 2006) that has been shown to be essential for T cell memory in response to acute infection and persistent LCMV infections (Jeannet et al., 2010; Zhao et al., 2010; Zhou et al., 2010; Utzschneider et al., 2016). In response to MCMV, it is also reexpressed by *Fx1*^{WT} T cells, but not by *Fx1*^{8KO} T cells (Fig. 5 A). Furthermore, because the T-box transcription factor EOMES is

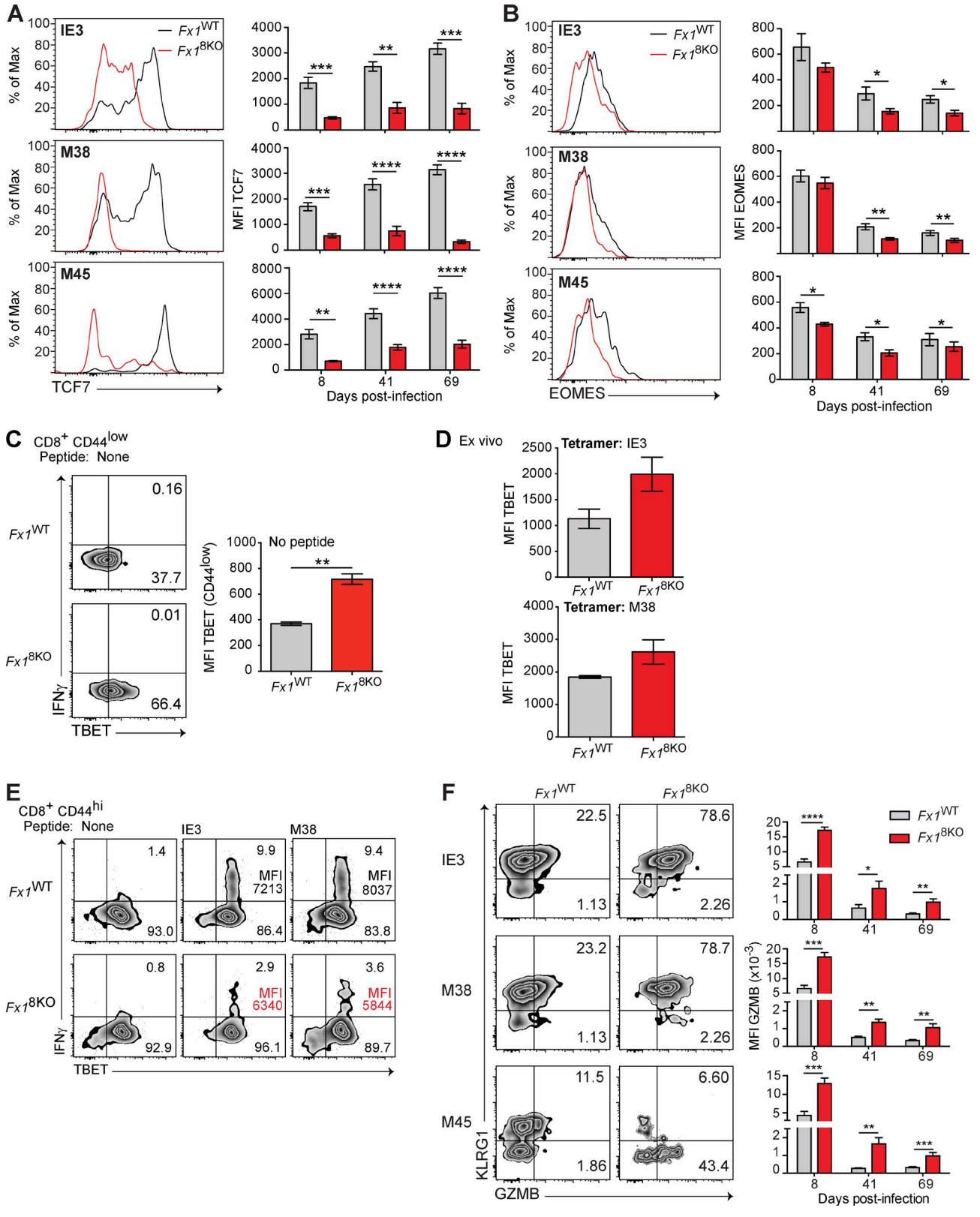

Figure 5. **Transcriptional control of MCMV–specific T cells is altered in the absence of FOXO1. (A and B)** TCF7 and EOMES MFI were determined on CD8+ tetramer+ cells for IE3, M38, and M45 epitopes. FACS histograms show TCF7 (A) and EOMES (B) MFI at 69 dpi. Quantification of EOMES and TCF7 MFI at 8, 41, and 69 dpi in the spleen of *Fx1*^{WT} and *Fx1*^{8KO} chimeras. Data are from one experiment for day 8 with $n = 4$ mice per group and cumulative from three

downstream of TCF7, it too is not normally up-regulated in *Fx1*^{8KO} T cells (Fig. 5 B).

Antigen-inexperienced *Fx1*^{8KO} T cells (CD8^{+}CD44^{lo}) from MCMV-infected chimeras expressed an amount of TBET that was low but higher than that of *Fx1*^{WT} T cells (Fig. 5 C). In addition, Ag-specific *Fx1*^{8KO} T cells expressed an increased amount of TBET compared with that of *Fx1*^{WT} T cells (Fig. 5 D), yet they were defective in the antigen-induced expression of IFNγ (Fig. 5 E). However, these TBET^{hi} T cells also exhibit characteristics of anergy, including the expression of EGR2 that interacts with TBET to diminish IFNγ transcription (Singh et al., 2017). The loss of TCF7 and EOMES and increase in TBET is consistent with a preferential effector-like phenotype of *Fx1*^{8KO} T cells as measured by the expression of GZMB over the course of the MCMV response (Fig. 5 F). Altogether, these data show that FOXO1 is needed for not only the induction of TCF7 and EOMES but also the repression of TBET. FOXO1 appears to tightly regulate these transcription factors in both long-lived effector/memory CD8^{+} T cells and inflationary CD8^{+} T cells.

Foxo1 is continuously required to maintain MCMV-specific memory T cell populations

To test the durability of the distinction between memory and effector cells, chimeras were infected, and after 30 d, *Foxo1* was deleted in CD8^{+} T cells by administration of tamoxifen. To clarify this model from the initial one, the chimeras are referred to as *L.Fx1*^{WT} and *L.Fx1*^{8KO} chimeras ("L" meaning late). Groups of mice were analyzed at day 40 (5 d after deletion) or day 56 (21 d after deletion; Fig. S4 A) for functional and transcriptional characteristics of memory and effector cells. These include the expression of BCL2, TCF7, EOMES, and GZMB, as well as the phenotypic characteristics of memory and effector cells, KLRG1, and CD27.

The number of cells specific for all three epitopes was diminished with the late loss of FOXO1 with the exception of T cells specific for M38 at the early time point (Fig. 6 A). By day 56, there was also a marked reversal of the functional and transcriptional memory characteristics prominently reflected by the loss of BCL2 (Fig. 6 B), a characteristic that suggests this was not a selectively surviving T cell population. In addition, there was a loss of TCF7 (Fig. 6 C and Fig. S4 B) and EOMES (Fig. S4 C), as well as the gain of GZMB expression (Fig. 6 D and Fig. S4 D). *Foxo1* deletion also correlated with a skewing of the proportion of cells expressing KLRG1 and CD27 (Fig. 6 E and Fig. S4 E). In addition to acquiring multiple phenotypic characteristics of effector cells, the postinfection inactivation of *Foxo1* also imbued the population with characteristics of anergy; that is, a loss of potential for cytokine production (Fig. 6 F) and a reduced binding of tetramers (Fig. 6 G and Figs. S4 F). To further characterize the effect of the late loss of FOXO1 on the CD8^{+} T cell response, we analyzed peripheral tissues and secondary lymphoid organs. After 21 d of FOXO1 inactivation, the MCMV-specific CD8^{+} T cell response was highly reduced in LNs, liver, lung, and blood (Fig. 7 A). This was accompanied by phenotypic changes for all three epitope-specific T cells, including reduced BCL2 (Fig. 7 B) and TCF7 expression (Fig. 7 C) and an increase in GZMB (Fig. 7 D). Interestingly, the loss of memory precursor KLRG1^{hi} CD27^{+} was also found in peripheral organs of *L.Fx1*^{8KO} chimeras (Fig. 7 E). Finally, consistent with T cells found in the spleen, MCMV-specific CD8^{+} T cells displayed characteristics of anergy: loss of effector cytokine production (Fig. 7 F) and reduction of tetramer binding (Fig. 7 G).

To determine whether CD8^{+} T cells deleted for *Foxo1* are functionally responsive, we performed two types of adoptive transfer experiments. In the first, *Fx*1^{WT} and *Fx1*^{8KO} chimeras were infected with MCMV for 21 d. The CD8^{+} CD44^{hi} KLRG1^{hi} CD27^{-} and KLRG1^{low} CD27^{+} cells were sorted (Fig. S5 A) and transferred into naive mice followed by MCMV infection to measure a secondary response. After 6 d, the memory and effector phenotype cells were enumerated (Fig. 8 A). As shown, CD27^{+} T cells displayed superior proliferative capacity compared with CD27^{-} T cells, and *Foxo1*^{WT} T cells were capable of at least 10-fold more expansion as compared with *Foxo1*^{8KO} T cells. This applied to T cells that recognized all three epitopes (Fig. 8 B).

Finally, to determine whether FOXO1 is required for a recall response after the differentiation of effector and memory T cells, the *Foxo1* gene was deleted 30 d after infection (Fig. S5 B) followed by an adoptive transfer (Fig. 8 C). With one exception, postinfection inactivation of *Foxo1* caused T cells specific for all three epitopes to become severely diminished in their capacity for proliferation in a recall response measured 7 or 21 d after infection (Fig. 8 D). The exception was again the T cell subset–specific M38 at 7 d after a secondary infection (see Discussion). Collectively, these data suggest

experiments for day 41 and day 69 with $n = 2$ to 5 mice per group and per experiment. **(C)** *Fx1*^{WT} and *Fx1*^{8KO} splenocytes were harvested at the indicated time points after infection, and splenocytes were cultured for 5 h without peptide stimulation. FACS plots represent the frequency of IFNγ and TBET at 41 dpi gated on CD8^{+} CD44^{low}. Quantification of TBET MFI on CD8^{+} CD44^{low} was determined. Numbers represent the percentage of TBET^{+} IFNγ^{+} or TBET^{+} IFNγ^{-}. Data are from one experiment with $n = 3$ mice per group. **(D)** Quantification of TBET MFI was examined ex vivo on CD8^{+} tetramer^{+} at 41 dpi. Data are from one experiment with $n = 3$ to 4 mice per group. **(E)** *Fx1*^{WT} and *Fx1*^{8KO} splenocytes were harvested at different time points after infection and splenocytes stimulated for 5 h with or without a specific peptide. FACS plots represent the frequency of IFNγ and TBET at 41 dpi gated on CD8^{+} CD44^{hi}. Numbers represent the IFNγ MFI among the TBET^{+} IFNγ^{+} cells and the percentage of TBET^{+} IFNγ^{+} or TBET^{+} IFNγ^{-}. Data are from one experiment with $n = 3$ to 4 mice per group. **(F)** Bivariant plots show the KLRG1 and GZMB expression at 41 dpi. Numbers represent the percentage of KLRG1^{+} GZMB^{+} and KLRG1^{-} GZMB^{+}. Graphs represent the GZMB MFI for the different time points and for each tetramer. Data are cumulative from two to four experiments with minimum $n = 3$ mice per group and per time point. *, $P < 0.05$; **, $P < 0.01$; ***, $P < 0.001$; ****, $P < 0.0001$ (unpaired Student's t test [A–D and F]); error bars represent mean ± SEM.

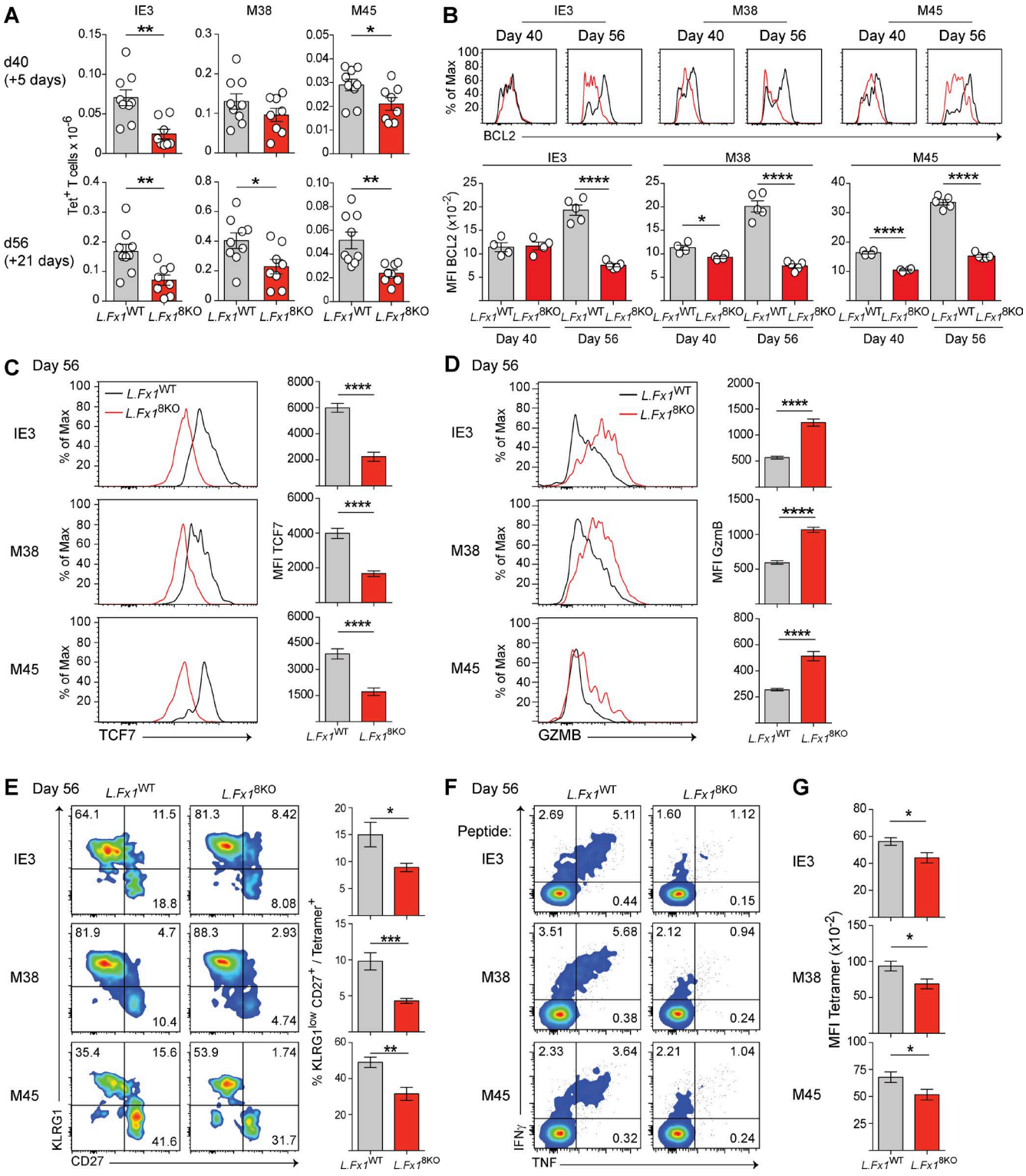

Figure 6. **Continued FOXO1 activity is crucial to maintain the survival and the differentiation state of MCMV-specific CD8⁺ T cells. (A–G)** Chimeras were treated with tamoxifen at day 30 after infection (Fig. S4 A) and analyzed either 5 or 21 d after inactivation of *Foxo1*. (A) Numbers of tetramer⁺ cells after 5 or 21 d of Foxo1 depletion. Data are cumulative from two experiments with $n = 3$ to 5 mice per group. (B) BCL2 expression for each tetramer and quantification is shown for one experiment representative of a total of two experiments with $n = 3$ to 5 mice per group. (C–G) Spleens were harvested 21 d after inactivation of *Foxo1*. (C) TCF7 expression was determined and the MFI plotted for T cells specific for each epitope. (D) GZMB expression was determined and the MFI plotted for T cells specific for each epitope. (E) Tetramer⁺ T cells were examined for the expression of KLRG1 and CD27, and the

that FOXO1 has to be continuously present to maintain the full characteristics of Ag-specific $CD8^+$ T cells after response to a persistent infection.

Inflation involves the FOXO1-dependent expression of TCF7

The immune response to CMV is unusual in the heterogeneity of responding T cells as illustrated by clonotypes specific for M45, M38, and IE3 epitopes. Nonetheless, all are dependent on FOXO1 for full elaboration, and as shown here and previously, FOXO1 is essential for postactivation TCF7 expression, required for the maintenance of T cell memory. We therefore sought to determine how loss of TCF7 expression would affect T cell subsets specific for different epitopes. Specifically, we determined the relative segregation of the $TCF7^+$ populations with respect to the expression of KLRG1.

As shown in Fig. 9 A, the $Fx1^{WT}$ T cells segregate as $KLRG1^{hi}$ $TCF7^-$ (typical of effector cells), $KLRG1^{hi}$ $TCF7^+$, and $KLRG1^-$ $TCF7^+$. With time, a majority of the $Fx1^{WT}$ $KLRG1^{hi}$ T cells become $TCF7^+$, a correlation that suggests a role for TCF7 in inflationary T cell responses. This phenomenon was also observed in the noninflationary M45-specific T cells (Fig. 9 A) and in an LCMV Armstrong infection (Delpoux et al., 2017). The $KLRG1^{hi}$ $TCF7^+$ cells express higher memory-associated molecules BCL2 and EOMES and exhibit diminished TBET expression compared with $KLRG1^{hi}$ $TCF7^-$ effector cells (Fig. 9 B). 5 d after inactivation of FOXO1, at the late stage of infection, we observed a diminished proportion of $KLRG1^{hi}$ $TCF7^+$ and $KLRG1^-$ $TCF7^+$ in the $L.Fx1^{8KO}$ T cells specific for the three epitopes (Fig. 9 C). This diminution increased with the length of FOXO1 inactivation, and it also occurred in T cells harvested from the lung (Fig. 9, C and D).

The population most strongly impacted by the deletion of FOXO1 was characterized as $KLRG1^{hi}$ $TCF7^+$. In an LCMV acute infection, $KLRG1^{hi}$ $CD127^+$ T cells appear, and they have a longer half-life compared with terminally differentiated $KLRG1^{hi}$ $CD127^-$ effector $CD8^+$ T cells (Cui and Kaech, 2010). This correlates with the observation that $KLRG1^{hi}$ $CD127^+$ $CD8^+$ T cells express higher amounts of TCF7 (Delpoux et al., 2017). Here, we show that the majority of $KLRG1^{hi}$ inflationary T cells express FOXO1-dependent, TCF7, and these cells increase with time. They may be a form of T_{EM} cells that are capable of long-term survival and the continuous production of $KLRG1^+$ effector cells. FOXO1 appears required for T cells to acquire and stabilize the effector memory phenotype, but it is also necessary to maintain $KLRG1^{hi}$ $TCF7^+$ MCMV-specific T cells associated with inflation.

DISCUSSION

Herpesviruses are cospeciated with their vertebrate hosts, meaning the host-pathogen relationship has coevolved, in some cases for hundreds of millions of years (McGeoch and Gatherer, 2005; Wang et al., 2007). Herpesviruses are never cleared, and they are thus adapted to infect and remain endemic in most or all vertebrates regardless of population size or density. As herpes family infections have been inevitable for most of vertebrate evolution, they may have also provided an important selection pressure for the development of the adaptive immune system. In particular, they may have contributed to the evolution of memory T cells that are self-renewing and can be continuously or periodically activated to expand and manifest effector functions.

In humans and mice, cytomegaloviruses induce strong epitope-specific T cell responses that follow distinctly different kinetics (Munks et al., 2006). At the extremes are T cells that rapidly expand and contract leaving behind typical central memory T cells, and T cells that gradually and continually expand with phenotypic characteristics of memory-effector T cells (Klenerman and Oxenius, 2016; Smith et al., 2016). We were interested to know whether these two distinctly different forms of memory have a common pathway of differentiation and maintenance.

The FOXO transcription factors are known to be important for cellular survival and organismal aging (Greer and Brunet, 2008; Martins et al., 2016). FOXO1 is essential for pluripotency for human and mouse embryonic stem cells, and it directly controls SOX2 and OCT4 expression, two of the four Yamanaka factors (Zhang et al., 2011; Takahashi and Yamanaka, 2016). It is also essential for the gene expression program associated with T cell memory as defined by the ability of T cells to be restimulated in a secondary response (Hess Michelini et al., 2013; Kim et al., 2013) or expand fully in a persistent viral infection (Staron et al., 2014).

Here, we show that T cells in which Foxo1 was deleted just before infection manifest a defective ability to accumulate that is caused by a deficiency in survival. T cell expansion was uniformly diminished at all stages of the response, and remarkably, the absence of FOXO1 did not affect the unique profiles of expansion and contraction for each of the three different epitope-specific responses measured. This loss could not be attributed to a difference in progression through the cell cycle; rather, it primarily resulted from increased cell death as measured by cleaved caspase-3 and cell-surface Annexin V. Importantly, the surviving *Foxo1*-null T cells were low for BCL2 expression, an indication that this population was not rescued by differential expression of survival fac-

quantification of the percentage of $KLRG1^{low}$ $CD27^+$ is shown. Numbers represent the percentage of $KLRG1^+$ $CD27^-$, $KLRG1^+$ $CD27^+$, and $KLRG1^-$ $CD27^+$. (F) Total splenocytes were stimulated for 5 h with a specific peptide and the proportion of IFNγ and TNF gated on $CD8^+$ $CD44^{hi}$ T cells are shown. Numbers represent the percentage of $IFN\gamma^+$ TNF^-, $IFN\gamma^+$ TNF^+, and $IFN\gamma^-$ TNF^+ T cells. (G) Histograms represent the tetramer MFI plotted for T cells specific for each epitope. Data in C–G are cumulative from two experiment with $n = 3$ to 5 mice per group. *, $P < 0.05$; **, $P < 0.01$; ***, $P < 0.001$; ****, $P < 0.0001$ (unpaired Student's *t* test [A–E and G]); error bars represent mean ± SEM.

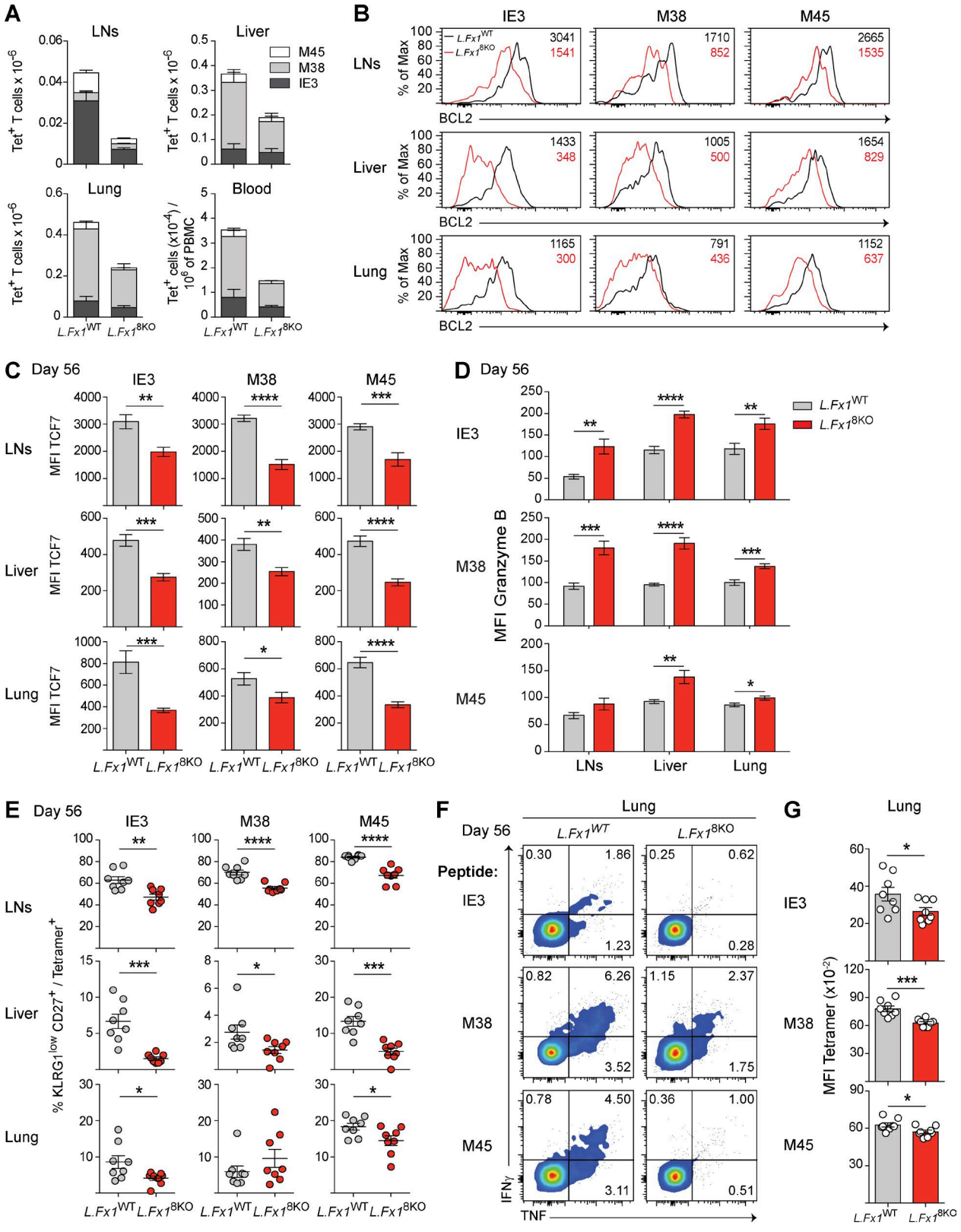

Figure 7. **Continued FOXO1 activity is crucial to maintain the survival and the differentiation state of MCMV-specific CD8⁺ T cells in blood, LNs, liver, and lungs. (A–G)** Chimeras were treated with tamoxifen at day 30 after infection (Fig. S4 A) and analyzed 21 d after inactivation of *Foxo1*. (A) Numbers of tetramer⁺ cells in LNs, blood, liver, and lungs. Data are cumulative from two experiment with $n = 4$ mice per group. (B) BCL2 expression for

tors. The likelihood is that the entire *Foxo1*-null population lost expression of BCL2 as a consequence of transition from memory to effector T cells.

The present study also describes an important role for FOXO1 to prevent the induction of anergy in Ag-specific $CD8^+$ T cells during a latent infection. One possibility is that the characteristics of anergy we noted (diminished tetramer avidity and calcium responses and enhanced ubiquitin ligases) in *Foxo1*-null T cells may also relate to the acquisition of an effector-like phenotype, especially under conditions of antigen persistence. Previous work showed that compared with central memory T cells, effector-memory cells express higher amounts of KLRG1 and have reduced avidity for MHC–peptide complexes due in part to an inhibitory signal delivered by KLRG1 (Griffiths et al., 2013). Still, the pathway involved in triggering the anergic state in Foxo1-null T cells is unknown.

The tendency to acquire an effector-like phenotype in the absence of FOXO1 was found to be continuously available to the antigen-specific responding T cells population. Inactivation of *Foxo1* after MCMV infection had effects similar or identical to that of inactivation before infection. There was loss of BCL2, TCF7, EOMES, and CD27, along with a gain of GZMB and KLRG1. These cells acquired an effector-like phenotype, but they were not capable effector cells because they were unable to produce a strong cytokine response. Either continued low-level antigen stimulation of effector cells causes a form of anergy or FOXO1 is required to maintain a full functional phenotype.

This raises the question of how FOXO1 is maintained as an active, nuclear, transcription factor in long-term memory cells. Comparing $KLRG1^+$ and $KLRG1^-$ T cells after either LCMV (Hess Michelini et al., 2013) or CMV infection shows that the amount of FOXO1 expressed is greater in $KLRG1^-$, effector-memory, or central memory T cells, and this level of regulation is possibly mediated by miR-150 (Ban et al., 2017). However, preliminary experiments show that the segregation of nuclear versus cytoplasmic FOXO1 in these subsets is equivalent (unpublished data). Although this suggests that memory versus effector phenotypes are regulated by relatively small changes in overall expression, the myriad posttranslational modifications of FOXO transcription factors are also likely to influence its activity and transcriptional specificity (Zhao et al., 2011).

Surprisingly, we found $Fx1^{8KO}$ M38 $tetramer^+$ cells, uniquely, did not decrease in number 5 d after *Foxo1* inactivation and retained a proliferative capacity after secondary challenge. This may correlate with the fact the M38 $Fx1^{WT}$ T cells express less TCF7 and FOXO1 than IE3 $CD8^+$ T cells (Figs. S4 B and S5 B); however, we do not understand the basis for a differential requirement for FOXO1 in IE3 and M38 T cells, and nothing is known regarding the sites or kinetics of M38 expression during MCMV infection in vivo that could provide insight. In summary, the present study reveals the profound requirements for FOXO1 in the diverse CMV-specific $CD8^+$ T cell response, including survival, differentiation, and function.

MATERIALS AND METHODS

Mice

C57BL/6 CD45.1 (CD45.1), C57BL/6 CD45.1/CD45.2 (CD45.1/CD45.2), C57BL/6 $CD8\alpha^{-/-}$, and C57BL/6 $TCR\alpha^{-/-}$ ($Tcra^{-/-}$) mice were bred in our colony at University of California, San Diego. $Foxo1^{f/f}$ mice were backcrossed to C57BL/6 (Jackson) for at least 13 generations and then crossed to $Rosa26^{Cre\text{-}ERT2}$, which had also been backcrossed to C57BL/6 for at least 14 generations. Id3-GFP mice are congenic with C57BL/6 mice. Mice were maintained in a specific pathogen–free vivarium. All experiments were performed in accordance to the Institutional Animal Care and Use Committee of University of California, San Diego.

Mixed bone marrow chimeras

Bone marrow cells were isolated from $CD8\alpha^{-/-}$, $Foxo1^{f/f}$ $Rosa26^{Cre\text{-}ERT2+}$, $Foxo1^{f/f}$ $Rosa26^{Cre\text{-}ERT2-}$, or CD45.1/CD45.2 mice and processed under sterile conditions. A single-cell suspension in PBS was obtained with a 1:1 ratio of $CD8\alpha^{-/-}$ and $Foxo1^{f/f}$ $Rosa26^{Cre\text{-}ERT2+}$ ($Fx1^{8KO}$ chimera) or $Foxo1^{f/f}$ $Rosa26^{Cre\text{-}ERT2-}$ ($Fx1^{WT}$ chimera) bone marrow cells. 5×10^6 cells were injected i.v. into lethally irradiated (10 gray) $TCR\alpha^{-/-}$ hosts in a volume of 200 µl. A second model of bone marrow transplantation was obtained by injecting a 1:1 ratio of CD45.1/CD45.2 and $Foxo1^{f/f}$ $Rosa26^{Cre\text{-}ERT2+}$ (CD45.2) bone marrow cells into lethally irradiated (10 gray) C57BL/6 CD45.1 hosts in a volume of 200 µl. Chimeras received autoclaved water treated with antibiotics (trimethoprim-sulfamethoxazole) until 4 wk after injection.

Tamoxifen treatment

After 8 wk of bone marrow transplantation, $Fx1^{8KO}$ and $Fx1^{WT}$ chimeras were injected every day for 5 d with 200 µl

each tetramer in LNs, liver, and lungs. Numbers represent the BCL2 MFI. Each FACS histogram is representative of two mice between two experiments with $n = 4$ mice per group and per experiment. (C) TCF7 expression was determined and the MFI plotted for T cells specific for each epitope in different organs. (D) GZMB expression was determined and the MFI plotted for T cells specific for each epitope in different organs. (E) $Tetramer^+$ cells were examined for the expression of KLRG1 and CD27, and the quantification of the percentage of $KLRG1^{low}$ $CD27^+$ T cells is shown. (F) Total lungs cells were stimulated for 5 h with a specific peptide and the proportion of IFNγ and TNF gated on $CD8^+$ $CD44^{hi}$ T cells are shown. Numbers represent the percentage of $IFN\gamma^+$ TNF^-, $IFN\gamma^+$ TNF^+ and $IFN\gamma^-$ TNF^+ T cells. (G) Histograms bars represent the tetramer MFI plotted for T cells specific for each epitope in the lungs. Data in A and C–G are cumulative from two experiments with $n = 8$ mice per group. *, $P < 0.05$; **, $P < 0.01$; ***, $P < 0.001$; ****, $P < 0.0001$ (unpaired Student's *t* test [C–E and G]); error bars represent mean ± SEM.

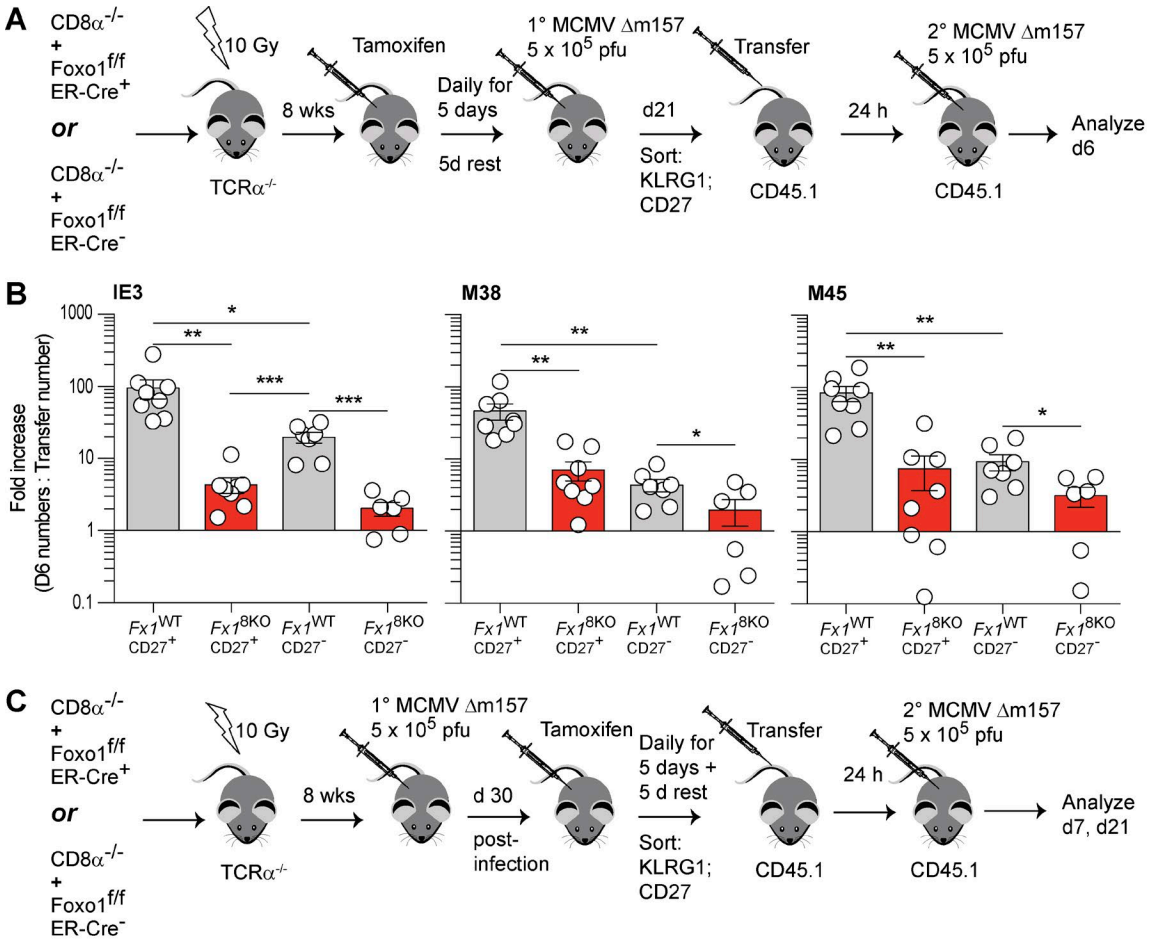
A
CD8α-/- + Foxo1f/f ER-Cre+
or
CD8α-/- + Foxo1f/f ER-Cre-
10 Gy
TCRα-/-
8 wks
Tamoxifen
Daily for 5 days
5d rest
1° MCMV Δm157 5 x 10^5 pfu
d21
Sort: KLRG1; CD27
Transfer
CD45.1
24 h
2° MCMV Δm157 5 x 10^5 pfu
CD45.1
Analyze d6
B
IE3
M38
M45
Fold increase (D6 numbers : Transfer number)
Fx1WT CD27+
Fx1 8KO CD27+
Fx1WT CD27-
Fx1 8KO CD27-
C
CD8α-/- + Foxo1f/f ER-Cre+
or
CD8α-/- + Foxo1f/f ER-Cre-
10 Gy
TCRα-/-
8 wks
1° MCMV Δm157 5 x 10^5 pfu
d 30 post-infection
Tamoxifen
Daily for 5 days + 5 d rest
Sort: KLRG1; CD27
Transfer
CD45.1
24 h
2° MCMV Δm157 5 x 10^5 pfu
CD45.1
Analyze d7, d21
D
IE3
M38
M45
Fold increase (d7 numbers : Transfer number)
L.Fx1WT CD27+
L.Fx1 8KO CD27+
L.Fx1WT CD27-
L.Fx1 8KO CD27-
Fold increase (d21 numbers : Transfer number)
L.Fx1WT CD27+
L.Fx1 8KO CD27+

tamoxifen (Cayman Chemicals) diluted in seed oil at 10 mg/ml. For late *Foxo1* inactivation, tamoxifen treatment began 30 d after infection.

Viral infections and plaque assay

Salivary gland stocks of MCMV Δm157 (McWhorter et al., 2013) were derived from the bacterial artificial chromosome–cloned MCMV strain K181 (Redwood et al., 2005), as previously described (Lio et al., 2016). *Fx1*^{8KO} and *Fx1*^{WT} chimeras were treated daily for 5 d with tamoxifen and after 5 d were infected with 5×10^5 PFU virus in 200 µl PBS i.p. At days 6, 8, 21, 41, 69, and 100 after infection, mice were killed by CO_2 asphyxiation and organs were harvested and immediately snap-frozen in liquid nitrogen. To determine viral titers, organs were weighed and homogenized, and serial dilutions of homogenates were added to monolayers of NIH-3T3 fibroblasts plated in 24-well plates. Plates were spun at 2,000 *g* for 10 min before incubation at 37°C, which increased the sensitivity of the plaque assays ∼6–10-fold. Cells were fixed with formalin, and plaques were visualized with 0.1% crystal violet and quantified.

Cell suspensions

Spleen and peripheral LNs were homogenized and passed through a nylon cell strainer in HBSS (Gibco) supplemented with 2% FBS or in 5% FBS, 0.1% NaN3 (Sigma-Aldrich) in PBS for flow cytometry. Blood samples were obtained by facial vein puncture. Liver was harvested after perfusion with PBS. The tissue was homogenized, and cells were then recovered after Percoll separation. Lungs were harvested after intracardiac perfusion with PBS. Lungs were cut in small pieces then mechanically dissociated and digested with 1 mg/ml collagenase D and 0.1 mg/ml DNase I (Roche) for 2 h at 37°C. The lungs were homogenized and passed through a nylon cell strainer in HBSS 2% FBS media. An ACK lysis buffer was applied on all cell suspensions and were resuspended in HBSS 2% FBS media.

Fluorescence staining and flow cytometry

Cell suspensions were collected and dispensed into 96-well round-bottom microtiter plates (4×10^6 cells/well). Surface staining was performed as previously describe. In brief, cells were incubated on ice (for 15 min per step) with Abs in 5% FCS, 0.1% NaN_3 (Sigma-Aldrich) PBS. Each cell-staining reaction was preceded by a 15-min incubation with a purified anti–mouse CD16/32 Ab (FcγRII/III block; 2.4G2). We used antibodies specific for CD4, CD8, CD11a, CD11b, CD11c, CD27, CD44, CTLA-4, Egr2, EOMES, FOXP3, KLRG1, LAG-3, PD-1, TCRβ, and Tim-3 from eBioscience. Rabbit anti–mouse TCF7 and FOXO1 (directly conjugated or not) and NFAT1 antibodies were from Cell Signaling. BCL2, PE-labeled GZMB, and FITC-Ki-67 antibodies are from BD Biosciences. APC-labeled GZMB was from Invitrogen. NFAT2, TBET, and XCR1 antibodies were from BioLegend. For E3 ubiquitin ligase staining, we used goat anti–Cbl-b (sc-1435) and rabbit anti-AIP4 (ITCH; sc-25625) from Santa Cruz Biotechnology and rabbit anti-RNF128 (Grail) from Abcam (ab137088). Secondary Alexa Fluor 647 donkey anti-rabbit (Invitrogen) was used to reveal FOXO1, Grail, ITCH, or TCF7 staining and secondary FITC donkey anti-goat (sc-2024) from Santa Cruz Biotechnology was used to reveal Cbl-b staining. For intracellular staining, the FOXP3 Staining Buffer Set (eBioscience) was used. BV421-labeled IE3, M38, and M45 tetramers were made and provided by National Institutes of Health tetramer core facilities (Atlanta, GA). Multicolor immunofluorescence was analyzed using a BD Fortessa and BD Fortessa X-20 cytometer (BD Biosciences). List-mode data files were analyzed using FlowJo Software.

Adoptive transfers and cell sorting

Splenocytes were harvested from *Fx1*^{WT} and *Fx1*^{8KO} chimeras or from *L.Fx1*^{WT} and *L.Fx1*^{8KO} chimeras. Total CD8$^+$ cells were enriched by negative selection with an EasySep Mouse CD8$^+$ T Cell Isolation kit (STEMCELL Technologies). Cells were stained with antibodies against CD8, CD27, CD44, and KLRG1, and a fraction of each sample was analyzed for the percentage of tetramer for IE3, M38, and M45 epitope. The CD8$^+$ CD44^{hi} KLRG1^{hi} CD27$^-$ and KLRG1^{low} CD27$^+$ cells were sorted on ARIA Fusion (BD Biosciences). Sort purity was checked on a BD Fortessa X-20. Sorted cells were counted, and 10^5 cells were transferred. The number of transferred tetramer-binding CD8$^+$ T cells was estimated using the tetramer frequency within the enriched CD8$^+$ population and the postsort purity analysis. Fold expansion was calculated as the number of tetramer-binding T cells in the spleen at various times after challenge over the total number of tetramer$^+$ cells transferred (assuming 10% engraftment).

Calcium measurement

2.5×10^6 splenocytes were resuspended in HBSS (phenol red free) with 1% FBS and 1 mM Ca^{2+} and Mg^{2+} plus 10 mM Hepes. Cells were loaded both Fluo-4 (Invitrogen) and Fura-Red (Invitrogen) mix dye for 45 min at 37°C. Cells were washed twice and stained for surface markers, and purified anti-CD3ε (clone 145-2C11; eBioscience) was added to the

Figure 8. **CD8$^+$ KLRG1^{low} CD27$^+$ *Fx1*^{8KO} fail to make a secondary response after inactivation of FOXO1. (A)** Model depicting the strategy used to measure a secondary response. **(B)** Fold expansion of CD8$^+$ tetramer$^+$ was determined 6 d after challenge. Data are cumulative from two transfer experiments with $n = 3$ or 4 mice per group and per experiment. **(C)** Model representing the secondary response after inactivation of *Foxo1* at day 30 after infection. **(D)** Fold expansion of CD8$^+$ tetramer$^+$ at day 7 and day 21 after challenge. Data are cumulative from two transfers experiment with $n = 3$ or 4 mice per group and per experiment. *, $P < 0.05$; **, $P < 0.01$; ***, $P < 0.001$; ****, $P < 0.0001$ (unpaired Student's *t* test [B and D]); error bars represent mean ± SEM.

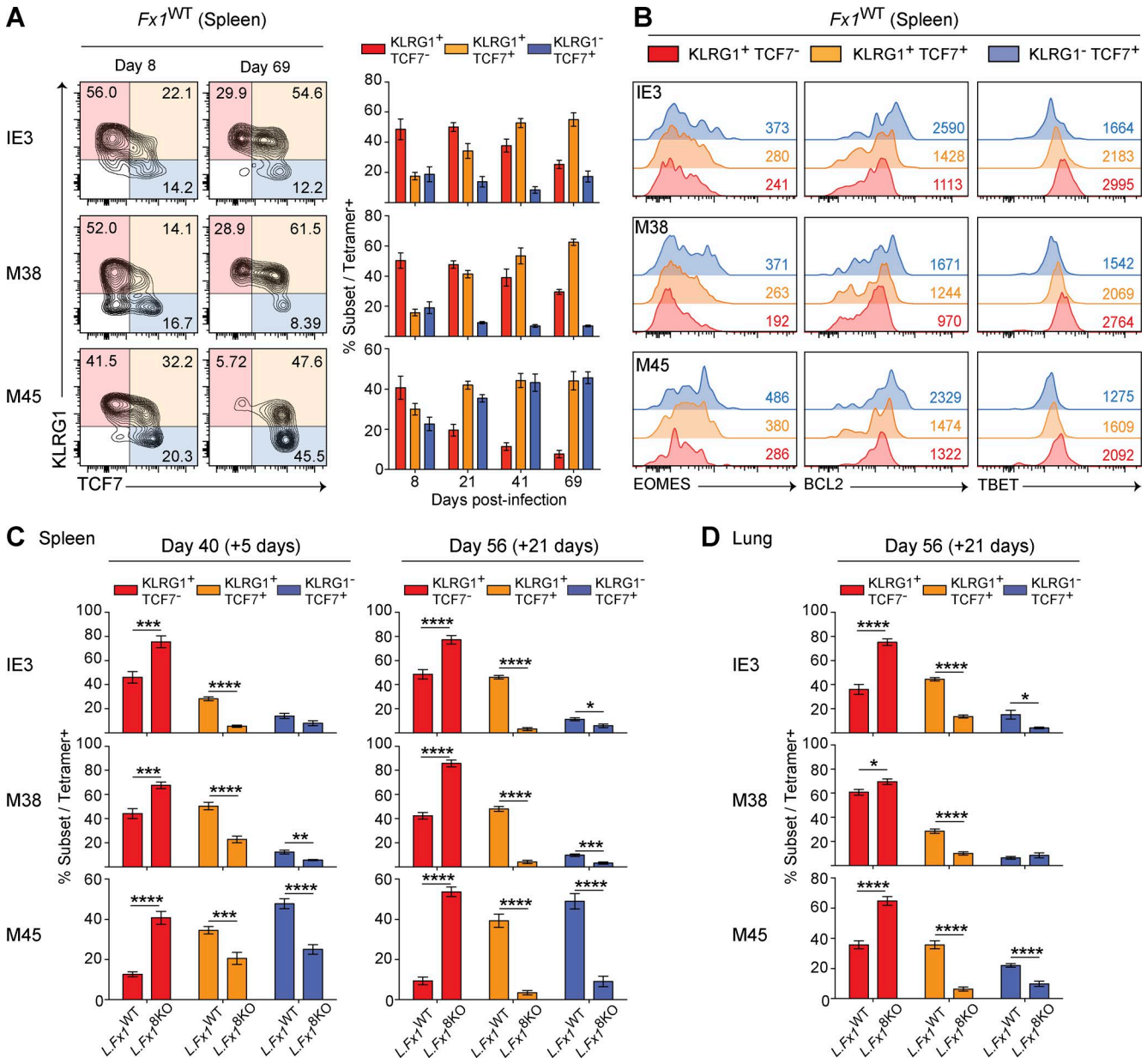

Figure 9. **FOXO1 maintains KLRG1$^+$ TCF7$^+$ effector-memory MCMV-CD8$^+$ T cells. (A–C)** *Fx1*^{WT} and *Fx1*^{8KO} splenocytes were harvested at indicated time points after infection. (A) Bivariant analysis of KLRG1 and TCF7 at 8 and 69 dpi gated on tetramer$^+$ cells (left) and each population were graphed for each time point (right) in *Fx1*^{WT} chimeras. Data are from one experiment for day 8 with $n = 4$ mice per group and cumulative from two experiments for day 21 and three experiments for day 41 and 69 with $n = 2–5$ mice per group and per experiment. (B) Numbers represent the percentage of KLRG1$^+$ TCF7$^-$, KLRG1$^+$ TCF7$^+$ and KLRG1$^-$ TCF7$^+$. EOMES, BCL2 and TBET expression is shown for each population and each tetramer at day 41 after infection in *Fx1*^{WT} chimeras. Numbers indicate the MFI of each molecule for each subset. **(C and D)** Chimeras were treated with tamoxifen at day 30 after infection and splenocytes were analyzed either 5 or 21 d after inactivation of *Foxo1*. Histograms show the proportion of the indicated population for each tetramer in the spleen (C) and lung (D) of *L.Fx1*^{WT} and *L.Fx1*^{8KO} chimeras. Data are cumulative from two experiments for each time point with $n = 8–9$ mice per group. *, $P < 0.05$; **, $P < 0.01$; ***, $P < 0.001$; ****, $P < 0.0001$ (unpaired Student's *t* test [C and D]); error bars represent mean ± SEM.

mix of antibodies. Samples were run at low speed, and purified anti-hamster was added to activate the cells after 30 s of acquisition on the Fortessa X-20 cytometer. Curves show ratio of Fluo-4 mean fluorescence intensity (MFI) and Fura-Red MFI over the time. The curves represent the CD8$^+$ CD44^{hi} CD11a^{hi} T cells gated on CD45.1$^+$ CD45.2$^+$ double-positive and CD45.2$^+$ CD45.1$^-$ for *Foxo1* WT and *Foxo1*-null cells, respectively.

Cytokine detection

To asses intracellular cytokine production, 2×10^6 splenocytes or lung cells were unstimulated or stimulated with 1 μg/ml IE3, M38, or M45 peptide and 10 μg/ml Monensin (eBioscience) for 5 h at 37°C. Cells were then stained for surface markers. Foxp3 Staining Buffer Set (eBioscience) was used for fixation and permeabilization, followed by labeling with specific cytokine Abs for IFNγ (clone XMG1.2) and TNF (clone MP6-XT22) from eBioscience.

Tetramer decay assay

The avidity of T cell populations was evaluated by decay of tetramer binding, as previously described (Wang and Altman, 2003). Splenocytes were harvested at day 41 after infection from *Fx1*^{8KO} and *Fx1*^{WT} chimeras. 4×10^6 splenocytes were stained with M38 tetramer for 30 min at 4°C in the presence of anti-CD8 mAb and anti-CD4 mAb. After three washes, anti-H-2Kb (clone Y-3) from BioXCell was added to a final concentration of 10 μM, and cells were removed at various time points and immediately fixed in 2% paraformaldehyde/PBS.

Proliferation assay

$CD8^+$ T cells were purified from spleen cells with STEM CELL total $CD8^+$ isolation kit as manufacturer's instructions. Cells were stained with 0.5 μM CFSE for 10 min at 37°C. Adding equal volume of FBS stopped the reaction. Cells were washed twice then counted. 0.2×10^6 cells per well were activated for 3 d at 37°C in 96-well plates previously coated with anti-CD3/anti-CD28. Proliferation index = $\log_2$ (f), where f = CFSE MFI (in the absence of stimulation)/CFSE MFI (in the presence of stimulation; Delpoux et al., 2012).

Apoptosis assay

For active caspase-3 detection, the CaspGlow Fluorescein Caspase-3 Staining kit (eBioscience) was used according to the manufacturer's instructions. In brief, cells from the spleen, LNs, and lung were stained for surface markers as described in the Fluorescence staining and flow cytometry section and cultured at 2×10^6 cells per well in complete media. 1 μl FITC-DEVD-FMK was added in 300 μl cells. Cells were washed twice and samples were acquired on cytometer. For some experiments, apoptosis was evaluated via flow cytometry using fluorescently conjugated Annexin V (BD Pharmingen). Upon the completion of surface staining, the splenocytes were washed and incubated in Annexin V binding buffer with Annexin V at a 1:20 dilution for 15 min at room temperature. The cells were then washed, resuspended in Annexin V binding buffer, and analyzed by flow cytometry immediately.

Statistical analysis

Prism 6 software (GraphPad) was used to analyze data by two-tailed unpaired or paired Student's *t* test (*, $P < 0.05$; **, $P < 0.01$; ***, $P < 0.001$; ****, $P < 0.0001$). Data are presented as means ± SEM.

Online supplemental material

Fig. S1 shows that only the $CD8^+$ T cell response is altered in *Fx1*^{8KO} mice and shows the FOXO1 deletion efficiency at day 8 and 69 after infection. Fig. S2 shows the increase apoptosis of MCMV-specific $CD8^+$ T cells in the liver, LNs, and lungs of *Fx1*^{8KO} mice. Fig. S3 shows that MCMV-specific $CD8^+$ T cells are not exhausted but display anergic phenotype. Fig. S4 depicts the model of late deletion of FOXO1 and the phenotype of MCMV-specific $CD8^+$ T cells after 5 d of deletion. Fig. S5 depicts the sorting strategy and the FOXO1 deletion efficiency after 5 d of the last tamoxifen treatment.

ACKNOWLEDGMENTS

We are grateful to the members of the Hedrick, Goldrath, and Benedict groups for helpful discussions and critical reading of the manuscript. We thank the members of Bruno Lucas group for technical advice and for manuscript discussion. We thank Andrew L. Doedens for comments, suggestions, and manuscript discussion.

This work was supported by the National Institutes of Health (grants R01AI037988 and R01AI103440 to S.M. Hedrick, grant AI1072117 to A.W. Goldrath, and grants AI101423 and AI113349 to C.A. Benedict).

The authors declare no competing financial interests.

Author contributions: A. Delpoux, R. Hess Michelini, C.A. Benedict, and S.M. Hedrick designed the experiments. A. Delpoux and R. Hess Michelini performed the experiments with technical help from S. Verma, C.-Y. Lai and D.T. Utzschneider. K.D. Omilusik performed the experiment on the ID3 GFP and A.W. Goldrath supervised the experiment. A.J. Redwood made the Δm157 MCMV virus. A. Delpoux and S.M. Hedrick wrote the manuscript with the assistance of all the other authors.

Submitted: 14 April 2017

Revised: 18 October 2017

Accepted: 6 December 2017

REFERENCES

Arase, H., E.S. Mocarski, A.E. Campbell, A.B. Hill, and L.L. Lanier. 2002. Direct recognition of cytomegalovirus by activating and inhibitory NK cell receptors. *Science.* 296:1323–1326. https://doi.org/10.1126/science.1070884

Ban, Y.H., S.C. Oh, S.H. Seo, S.M. Kim, I.P. Choi, P.D. Greenberg, J. Chang, T.D. Kim, and S.J. Ha. 2017. miR-150-Mediated Foxo1 Regulation Programs CD8+ T Cell Differentiation. *Cell Reports.* 20:2598–2611. https://doi.org/10.1016/j.celrep.2017.08.065

Barathan, M., K. Gopal, R. Mohamed, R. Ellegård, A. Saeidi, J. Vadivelu, A.W. Ansari, H.A. Rothan, M. Ravishankar Ram, K. Zandi, et al. 2015. Chronic hepatitis C virus infection triggers spontaneous differential expression of biosignatures associated with T cell exhaustion and apoptosis signaling in peripheral blood mononucleocytes. *Apoptosis.* 20:466–480. https://doi.org/10.1007/s10495-014-1084-y

Betts, M.R., M.C. Nason, S.M. West, S.C. De Rosa, S.A. Migueles, J. Abraham, M.M. Lederman, J.M. Benito, P.A. Goepfert, M. Connors, et al. 2006. HIV nonprogressors preferentially maintain highly functional HIV-specific CD8+ T cells. *Blood.* 107:4781–4789. https://doi.org/10.1182/blood-2005-12-4818

Borst, J., J. Hendriks, and Y. Xiao. 2005. CD27 and CD70 in T cell and B cell activation. *Curr. Opin. Immunol.* 17:275–281. https://doi.org/10.1016/j.coi.2005.04.004

Brown, M.G., A.A. Scalzo, L.R. Stone, P.Y. Clark, Y. Du, B. Palanca, and W.M. Yokoyama. 2001. Natural killer gene complex (Nkc) allelic variability in

inbred mice: evidence for Nkc haplotypes. *Immunogenetics.* 53:584–591. https://doi.org/10.1007/s002510100365

Brunet, A., A. Bonni, M.J. Zigmond, M.Z. Lin, P. Juo, L.S. Hu, M.J. Anderson, K.C. Arden, J. Blenis, and M.E. Greenberg. 1999. Akt promotes cell survival by phosphorylating and inhibiting a Forkhead transcription factor. *Cell.* 96:857–868. https://doi.org/10.1016/S0092-8674(00)80595-4

Calnan, D.R., and A. Brunet. 2008. The FoxO code. *Oncogene.* 27:2276–2288. https://doi.org/10.1038/onc.2008.21

Chang, J.T., V.R. Palanivel, I. Kinjyo, F. Schambach, A.M. Intlekofer, A. Banerjee, S.A. Longworth, K.E. Vinup, P. Mrass, J. Oliaro, et al. 2007. Asymmetric T lymphocyte division in the initiation of adaptive immune responses. *Science.* 315:1687–1691. https://doi.org/10.1126/science.1139393

Clevers, H. 2006. Wnt/beta-catenin signaling in development and disease. *Cell.* 127:469–480. https://doi.org/10.1016/j.cell.2006.10.018

Cui, W., and S.M. Kaech. 2010. Generation of effector CD8+ T cells and their conversion to memory T cells. *Immunol. Rev.* 236:151–166. https://doi.org/10.1111/j.1600-065X.2010.00926.x

Day, C.L., D.E. Kaufmann, P. Kiepiela, J.A. Brown, E.S. Moodley, S. Reddy, E.W. Mackey, J.D. Miller, A.J. Leslie, C. DePierres, et al. 2006. PD-1 expression on HIV-specific T cells is associated with T-cell exhaustion and disease progression. *Nature.* 443:350–354. https://doi.org/10.1038/nature05115

Delpoux, A., M. Poitrasson-Rivière, A. Le Campion, A. Pommier, P. Yakonowsky, S. Jacques, F. Letourneur, C. Randriamampita, B. Lucas, and C. Auffray. 2012. Foxp3-independent loss of regulatory CD4+ T-cell suppressive capacities induced by self-deprivation. *Eur. J. Immunol.* 42:1237–1249. https://doi.org/10.1002/eji.201142148

Delpoux, A., C.Y. Lai, S.M. Hedrick, and A.L. Doedens. 2017. FOXO1 opposition of CD8+ T cell effector programming confers early memory properties and phenotypic diversity. *Proc. Natl. Acad. Sci. USA.* 114:E8865–E8874. https://doi.org/10.1073/pnas.1618916114

Drake, D.R. III, R.M. Ream, C.W. Lawrence, and T.J. Braciale. 2005. Transient loss of MHC class I tetramer binding after CD8+ T cell activation reflects altered T cell effector function. *J. Immunol.* 175:1507–1515. https://doi.org/10.4049/jimmunol.175.3.1507

Dubois, P.M., M. Pihlgren, M. Tomkowiak, M. Van Mechelen, and J. Marvel. 1998. Tolerant CD8 T cells induced by multiple injections of peptide antigen show impaired TCR signaling and altered proliferative responses in vitro and in vivo. *J. Immunol.* 161:5260–5267.

Gerdes, J., H. Lemke, H. Baisch, H.H. Wacker, U. Schwab, and H. Stein. 1984. Cell cycle analysis of a cell proliferation-associated human nuclear antigen defined by the monoclonal antibody Ki-67. *J. Immunol.* 133:1710–1715.

Gigley, J.P., R. Bhadra, M.M. Moretto, and I.A. Khan. 2012. T cell exhaustion in protozoan disease. *Trends Parasitol.* 28:377–384. https://doi.org/10.1016/j.pt.2012.07.001

Greer, E.L., and A. Brunet. 2008. FOXO transcription factors in ageing and cancer. *Acta Physiol. (Oxf.).* 192:19–28. https://doi.org/10.1111/j.1748-1716.2007.01780.x

Griffiths, S.J., N.E. Riddell, J. Masters, V. Libri, S.M. Henson, A. Wertheimer, D. Wallace, S. Sims, L. Rivino, A. Larbi, et al. 2013. Age-associated increase of low-avidity cytomegalovirus-specific CD8+ T cells that re-express CD45RA. *J. Immunol.* 190:5363–5372. https://doi.org/10.4049/jimmunol.1203267

Hess Michelini, R., A.L. Doedens, A.W. Goldrath, and S.M. Hedrick. 2013. Differentiation of CD8 memory T cells depends on Foxo1. *J. Exp. Med.* 210:1189–1200. https://doi.org/10.1084/jem.20130392

Jeannet, G., C. Boudousquié, N. Gardiol, J. Kang, J. Huelsken, and W. Held. 2010. Essential role of the Wnt pathway effector Tcf-1 for the establishment of functional CD8 T cell memory. *Proc. Natl. Acad. Sci. USA.* 107:9777–9782. https://doi.org/10.1073/pnas.0914127107

Jeon, M.S., A. Atfield, K. Venuprasad, C. Krawczyk, R. Sarao, C. Elly, C. Yang, S. Arya, K. Bachmaier, L. Su, et al. 2004. Essential role of the E3 ubiquitin ligase Cbl-b in T cell anergy induction. *Immunity.* 21:167–177. https://doi.org/10.1016/j.immuni.2004.07.013

Kerdiles, Y.M., E.L. Stone, D.R. Beisner, M.A. McGargill, I.L. Ch'en, C. Stockmann, C.D. Katayama, and S.M. Hedrick. 2010. Foxo transcription factors control regulatory T cell development and function. *Immunity.* 33:890–904. https://doi.org/10.1016/j.immuni.2010.12.002

Kill, I.R. 1996. Localisation of the Ki-67 antigen within the nucleolus. Evidence for a fibrillarin-deficient region of the dense fibrillar component. *J. Cell Sci.* 109:1253–1263.

Kim, M.V., W. Ouyang, W. Liao, M.Q. Zhang, and M.O. Li. 2013. The transcription factor Foxo1 controls central-memory CD8+ T cell responses to infection. *Immunity.* 39:286–297. https://doi.org/10.1016/j.immuni.2013.07.013

Klenerman, P., and A. Hill. 2005. T cells and viral persistence: lessons from diverse infections. *Nat. Immunol.* 6:873–879. https://doi.org/10.1038/ni1241

Klenerman, P., and A. Oxenius. 2016. T cell responses to cytomegalovirus. *Nat. Rev. Immunol.* 16:367–377. https://doi.org/10.1038/nri.2016.38

Kurtulus, S., P. Tripathi, M.E. Moreno-Fernandez, A. Sholl, J.D. Katz, H.L. Grimes, and D.A. Hildeman. 2011. Bcl-2 allows effector and memory CD8+T cells to tolerate higher expression of Bim. *J. Immunol.* 186:5729–5737. https://doi.org/10.4049/jimmunol.1100102

Lio, C.W., B. McDonald, M. Takahashi, R. Dhanwani, N. Sharma, J. Huang, E. Pham, C.A. Benedict, and S. Sharma. 2016. cGAS-STING Signaling Regulates Initial Innate Control of Cytomegalovirus Infection. *J. Virol.* 90:7789–7797. https://doi.org/10.1128/JVI.01040-16

Maeda, Y., H. Nishikawa, D. Sugiyama, D. Ha, M. Hamaguchi, T. Saito, M. Nishioka, J.B. Wing, D. Adeegbe, I. Katayama, and S. Sakaguchi. 2014. Detection of self-reactive $CD8^+$ T cells with an anergic phenotype in healthy individuals. *Science.* 346:1536–1540. https://doi.org/10.1126/science.aaa1292

Mallone, R., S.A. Kochik, H. Reijonen, B. Carson, S.F. Ziegler, W.W. Kwok, and G.T. Nepom. 2005. Functional avidity directs T-cell fate in autoreactive CD4+ T cells. *Blood.* 106:2798–2805. https://doi.org/10.1182/blood-2004-12-4848

Martins, R., G.J. Lithgow, and W. Link. 2016. Long live FOXO: unraveling the role of FOXO proteins in aging and longevity. *Aging Cell.* 15:196–207. https://doi.org/10.1111/acel.12427

Masopust, D., V. Vezys, A.L. Marzo, and L. Lefrançois. 2001. Preferential localization of effector memory cells in nonlymphoid tissue. *Science.* 291:2413–2417. https://doi.org/10.1126/science.1058867

McGeoch, D.J., and D. Gatherer. 2005. Integrating reptilian herpesviruses into the family herpesviridae. *J. Virol.* 79:725–731. https://doi.org/10.1128/JVI.79.2.725-731.2005

McWhorter, A.R., L.M. Smith, L.L. Masters, B. Chan, G.R. Shellam, and A.J. Redwood. 2013. Natural killer cell dependent within-host competition arises during multiple MCMV infection: consequences for viral transmission and evolution. *PLoS Pathog.* 9:e1003111. https://doi.org/10.1371/journal.ppat.1003111

Munks, M.W., K.S. Cho, A.K. Pinto, S. Sierro, P. Klenerman, and A.B. Hill. 2006. Four distinct patterns of memory CD8 T cell responses to chronic murine cytomegalovirus infection. *J. Immunol.* 177:450–458. https://doi.org/10.4049/jimmunol.177.1.450

Obar, J.J., and L. Lefrançois. 2010. Memory CD8+ T cell differentiation. *Ann. N. Y. Acad. Sci.* 1183:251–266. https://doi.org/10.1111/j.1749-6632.2009.05126.x

Oh, Y.M., H.B. Park, J.H. Shin, J.E. Lee, H.Y. Park, D.H. Kho, J.S. Lee, H. Choi, T. Okuda, K. Kokame, et al. 2015. Ndrg1 is a T-cell clonal anergy factor negatively regulated by CD28 costimulation and interleukin-2. *Nat. Commun.* 6:8698. https://doi.org/10.1038/ncomms9698

Peck, B., E.C. Ferber, and A. Schulze. 2013. Antagonism between FOXO and MYC Regulates Cellular Powerhouse. *Front. Oncol.* 3:96. https://doi.org/10.3389/fonc.2013.00096

Pollizzi, K.N., I.H. Sun, C.H. Patel, Y.C. Lo, M.H. Oh, A.T. Waickman, A.J. Tam, R.L. Blosser, J. Wen, G.M. Delgoffe, and J.D. Powell. 2016. Asymmetric inheritance of mTORC1 kinase activity during division dictates CD8(+) T cell differentiation. *Nat. Immunol.* 17:704–711. https://doi.org/10.1038/ni.3438

Rao, R.R., Q. Li, M.R. Gubbels Bupp, and P.A. Shrikant. 2012. Transcription factor Foxo1 represses T-bet-mediated effector functions and promotes memory CD8(+) T cell differentiation. *Immunity.* 36:374–387. https://doi.org/10.1016/j.immuni.2012.01.015

Redwood, A.J., M. Messerle, N.L. Harvey, C.M. Hardy, U.H. Koszinowski, M.A. Lawson, and G.R. Shellam. 2005. Use of a murine cytomegalovirus K181-derived bacterial artificial chromosome as a vaccine vector for immunocontraception. *J. Virol.* 79:2998–3008. https://doi.org/10.1128/JVI.79.5.2998-3008.2005

Rutishauser, R.L., and S.M. Kaech. 2010. Generating diversity: transcriptional regulation of effector and memory CD8 T-cell differentiation. *Immunol. Rev.* 235:219–233. https://doi.org/10.1111/j.0105-2896.2010.00901.x

Safford, M., S. Collins, M.A. Lutz, A. Allen, C.T. Huang, J. Kowalski, A. Blackford, M.R. Horton, C. Drake, R.H. Schwartz, and J.D. Powell. 2005. Egr-2 and Egr-3 are negative regulators of T cell activation. *Nat. Immunol.* 6:472–480. https://doi.org/10.1038/ni1193

Sallusto, F., J. Geginat, and A. Lanzavecchia. 2004. Central memory and effector memory T cell subsets: function, generation, and maintenance. *Annu. Rev. Immunol.* 22:745–763. https://doi.org/10.1146/annurev.immunol.22.012703.104702

Scalzo, A.A., M. Manzur, C.A. Forbes, M.G. Brown, and G.R. Shellam. 2005. NK gene complex haplotype variability and host resistance alleles to murine cytomegalovirus in wild mouse populations. *Immunol. Cell Biol.* 83:144–149. https://doi.org/10.1111/j.1440-1711.2005.01311.x

Seckert, C.K., M. Griessl, J.K. Büttner, S. Scheller, C.O. Simon, K.A. Kropp, A. Renzaho, B. Kühnapfel, N.K. Grzimek, and M.J. Reddehase. 2012. Viral latency drives 'memory inflation': a unifying hypothesis linking two hallmarks of cytomegalovirus infection. *Med. Microbiol. Immunol. (Berl.).* 201:551–566. https://doi.org/10.1007/s00430-012-0273-y

Singh, R., T. Miao, A.L.J. Symonds, B. Omodho, S. Li, and P. Wang. 2017. Egr2 and 3 Inhibit T-bet-Mediated IFN-γ Production in T Cells. *J. Immunol.* 198:4394–4402. https://doi.org/10.4049/jimmunol.1602010

Smith, C.J., M. Quinn, and C.M. Snyder. 2016. CMV-Specific CD8 T Cell Differentiation and Localization: Implications for Adoptive Therapies. *Front. Immunol.* 7:352. https://doi.org/10.3389/fimmu.2016.00352

Smith, H.R., J.W. Heusel, I.K. Mehta, S. Kim, B.G. Dorner, O.V. Naidenko, K. Iizuka, H. Furukawa, D.L. Beckman, J.T. Pingel, et al. 2002. Recognition of a virus-encoded ligand by a natural killer cell activation receptor. *Proc. Natl. Acad. Sci. USA.* 99:8826–8831. https://doi.org/10.1073/pnas.092258599

Staron, M.M., S.M. Gray, H.D. Marshall, I.A. Parish, J.H. Chen, C.J. Perry, G. Cui, M.O. Li, and S.M. Kaech. 2014. The transcription factor FoxO1 sustains expression of the inhibitory receptor PD-1 and survival of antiviral CD8(+) T cells during chronic infection. *Immunity.* 41:802–814. https://doi.org/10.1016/j.immuni.2014.10.013

Steinert, E.M., J.M. Schenkel, K.A. Fraser, L.K. Beura, L.S. Manlove, B.Z. Igyártó, P.J. Southern, and D. Masopust. 2015. Quantifying Memory CD8 T Cells Reveals Regionalization of Immunosurveillance. *Cell.* 161:737–749. https://doi.org/10.1016/j.cell.2015.03.031

Takahashi, K., and S. Yamanaka. 2016. A decade of transcription factor-mediated reprogramming to pluripotency. *Nat. Rev. Mol. Cell Biol.* 17:183–193. https://doi.org/10.1038/nrm.2016.8

Tan, P., H. Guan, L. Xie, B. Mi, Z. Fang, J. Li, and F. Li. 2015. FOXO1 inhibits osteoclastogenesis partially by antagnozing MYC. *Sci. Rep.* 5:16835. https://doi.org/10.1038/srep16835

Urbani, S., B. Amadei, D. Tola, M. Massari, S. Schivazappa, G. Missale, and C. Ferrari. 2006. PD-1 expression in acute hepatitis C virus (HCV) infection is associated with HCV-specific CD8 exhaustion. *J. Virol.* 80:11398–11403. https://doi.org/10.1128/JVI.01177-06

Utzschneider, D.T., M. Charmoy, V. Chennupati, L. Pousse, D.P. Ferreira, S. Calderon-Copete, M. Danilo, F. Alfei, M. Hofmann, D. Wieland, et al. 2016. T Cell Factor 1-Expressing Memory-like CD8(+) T Cells Sustain the Immune Response to Chronic Viral Infections. *Immunity.* 45:415–427. https://doi.org/10.1016/j.immuni.2016.07.021

Verbist, K.C., C.S. Guy, S. Milasta, S. Liedmann, M.M. Kamiński, R. Wang, and D.R. Green. 2016. Metabolic maintenance of cell asymmetry following division in activated T lymphocytes. *Nature.* 532:389–393. https://doi.org/10.1038/nature17442

Wang, X.L., and J.D. Altman. 2003. Caveats in the design of MHC class I tetramer/antigen-specific T lymphocytes dissociation assays. *J. Immunol. Methods.* 280:25–35. https://doi.org/10.1016/S0022-1759(03)00079-6

Wang, N., P.F. Baldi, and B.S. Gaut. 2007. Phylogenetic analysis, genome evolution and the rate of gene gain in the Herpesviridae. *Mol. Phylogenet. Evol.* 43:1066–1075. https://doi.org/10.1016/j.ympev.2006.11.019

Welten, S.P., A. Redeker, K.L. Franken, J.D. Oduro, F. Ossendorp, L. Čičin-Šain, C.J. Melief, P. Aichele, and R. Arens. 2015. The viral context instructs the redundancy of costimulatory pathways in driving CD8(+) T cell expansion. *eLife.* 4. https://doi.org/10.7554/eLife.07486

Wherry, E.J., J.N. Blattman, K. Murali-Krishna, R. van der Most, and R. Ahmed. 2003. Viral persistence alters CD8 T-cell immunodominance and tissue distribution and results in distinct stages of functional impairment. *J. Virol.* 77:4911–4927. https://doi.org/10.1128/JVI.77.8.4911-4927.2003

Wherry, E.J., S.J. Ha, S.M. Kaech, W.N. Haining, S. Sarkar, V. Kalia, S. Subramaniam, J.N. Blattman, D.L. Barber, and R. Ahmed. 2007. Molecular signature of CD8+ T cell exhaustion during chronic viral infection. *Immunity.* 27:670–684. https://doi.org/10.1016/j.immuni.2007.09.006

Whiting, C.C., L.L. Su, J.T. Lin, and C.G. Fathman. 2011. GRAIL: a unique mediator of CD4 T-lymphocyte unresponsiveness. *FEBS J.* 278:47–58. https://doi.org/10.1111/j.1742-4658.2010.07922.x

Wilhelm, K., K. Happel, G. Eelen, S. Schoors, M.F. Oellerich, R. Lim, B. Zimmermann, I.M. Aspalter, C.A. Franco, T. Boettger, et al. 2016. FOXO1 couples metabolic activity and growth state in the vascular endothelium. *Nature.* 529:216–220. https://doi.org/10.1038/nature16498

Wojciechowski, S., P. Tripathi, T. Bourdeau, L. Acero, H.L. Grimes, J.D. Katz, F.D. Finkelman, and D.A. Hildeman. 2007. Bim/Bcl-2 balance is critical for maintaining naive and memory T cell homeostasis. *J. Exp. Med.* 204:1665–1675. https://doi.org/10.1084/jem.20070618

Yang, C.Y., J.A. Best, J. Knell, E. Yang, A.D. Sheridan, A.K. Jesionek, H.S. Li, R.R. Rivera, K.C. Lind, L.M. D'Cruz, et al. 2011. The transcriptional regulators Id2 and Id3 control the formation of distinct memory CD8+ T cell subsets. *Nat. Immunol.* 12:1221–1229. https://doi.org/10.1038/ni.2158

Zajac, A.J., J.N. Blattman, K. Murali-Krishna, D.J. Sourdive, M. Suresh, J.D. Altman, and R. Ahmed. 1998. Viral immune evasion due to persistence of activated T cells without effector function. *J. Exp. Med.* 188:2205–2213. https://doi.org/10.1084/jem.188.12.2205

Zehn, D., D.T. Utzschneider, and R. Thimme. 2016. Immune-surveillance through exhausted effector T-cells. *Curr. Opin. Virol.* 16:49–54. https://doi.org/10.1016/j.coviro.2016.01.002

Zhang, X., S. Yalcin, D.F. Lee, T.Y. Yeh, S.M. Lee, J. Su, S.K. Mungamuri, P. Rimmelé, M. Kennedy, R. Sellers, et al. 2011. FOXO1 is an essential regulator of pluripotency in human embryonic stem cells. *Nat. Cell Biol.* 13:1092–1099. https://doi.org/10.1038/ncb2293

Zhao, D.M., S. Yu, X. Zhou, J.S. Haring, W. Held, V.P. Badovinac, J.T. Harty, and H.H. Xue. 2010. Constitutive activation of Wnt signaling favors generation of memory CD8 T cells. *J. Immunol.* 184:1191–1199. https://doi.org/10.4049/jimmunol.0901199

Zhao, Y., Y. Wang, and W.G. Zhu. 2011. Applications of post-translational modifications of FoxO family proteins in biological functions. *J. Mol. Cell Biol.* 3:276–282. https://doi.org/10.1093/jmcb/mjr013

Zhou, X., S. Yu, D.M. Zhao, J.T. Harty, V.P. Badovinac, and H.H. Xue. 2010. Differentiation and persistence of memory CD8(+) T cells depend on T cell factor 1. *Immunity.* 33:229–240. https://doi.org/10.1016/j.immuni.2010.08.002